STRUCTURAL INTEGRITY Associates, Inc.	CALCULATION PACKAGE	FILE No.: TRW-06Q-319 PROJECT No.: TRW-06Q

PROJECT NAME: Optimization of the Weld Process and Mitigation Processes for Waste Package Stress Minimization

CLIENT: Bechtel SAIC Company, LLC

CALCULATION TITLE: Residual Stress Analyses on the 21 PWR Mockup Waste Package Outer Shell Due to Quenching and General Corrosion Using a Side-wall Thickness of 20mm

Document Revision	Affected Pages	Revision Description	Project Mgr. Approval Signature & Date	Preparer(s) & Checker(s) Signatures & Date
0	1-34 A1 In Computer Files	Original Issue	Marcos Herrera MLH 06/28/02	Francis Ku FHK 06/28/02 Stan Tang SST 06/28/02
1	1-72 A1 In Computer Files	Incorporated major client comments. Added analysis using BKIN curves. Added corrosion evaluations and K calculations for all analyses. Deleted Reference 3.	8/15/02	FHK 08/15/02 8/15/02

Table of Contents

1.0 INTRODUCTION

This calculation determines the residual stresses due to solution anneal and quenching of the 21 PWR Mockup Waste Package container outer shell using a side-wall thickness of 20 *mm*. The effects on the stresses due to general corrosion on the outside surface of the Mockup Waste Package outer shell are also evaluated. In addition, analysis is performed to evaluate the effects between outside surface quenching and inside and outside surface quenching to the residual stress distribution, as well as the effects between bilinear isotropic hardening and bilinear kinematic hardening properties for the outer shell material.

2.0 TECHNICAL APPROACH

This calculation continues from a previous calculation package [1] to evaluate the residual stress analysis on the 21 PWR Mockup Waste Package (MWP) container shell. The geometric and analytical inputs are obtained from Reference 1, with one modification to the thickness of the middle wall section being thinner at 20 *mm*, while the model in Reference 1 has a mid-wall thickness of 25 *mm*. Also, the hardening characteristics of the material can affect the resultant residual stress distribution. Therefore, analysis is also performed to evaluate the difference between bilinear isotropic hardening (BISO) and bilinear kinematic hardening (BKIN).

In addition, it is determined that the tangent modulii (E_t) for the material, which are the slopes of the plastic region of the stress-strain curves at different temperatures, used in Reference 1 are over-conservative; they are: E_t = 0.41% of E at 20°C, and E_t = 0.13% of E at 1120°C. Therefore, the tangent modulii are scaled up by a factor of 5 for better solution convergence during the analysis, and the maximum factored E_t is only 2.05% of E, which remains very small. This adjustment is appropriate because, in reality, the transition to plasticity is smooth and the model does not expected to achieve large strain under the applied loads. The finite element model for the thinned MWP outer shell is shown in Figure 1, and the adjusted material properties for the material is shown in Figure 2. Note that Figure 2 shows the BISO curves, the BKIN curves for the material is identical to the BISO curves, only with different curve types assigned to ANSYS [2].

Due to general corrosion that can occur, material that is subjected to compressive stress at the beginning of service will corrode away. Loss of this material will cause the residual stress to redistribute since equilibrium must exist. Thus, an analysis is required to determine the redistribution of residual stress with time as general corrosion occurs.

3.0 LOSS OF MATERIAL DUE TO GENERAL CORROSION

The effect of corrosion is simulated by eliminating the outer layer elements on the outside surface of the MWP outer shell, with the thickness of the layer equal to the thickness of one element. For this analysis, layers of elements are removed from the outside surface to simulate gradual corrosion, and the thickness for each element (layer) is approximately 2.00 *mm*.

As shown in Figure 1, four sections are selected for consideration in this analysis. These sections correspond to the critical location in the MWP wall. They are considered critical because of the geometry and expected behavior of the MWP. It is confirmed later that these four sections include the limiting locations based on tensile stresses on the outside surface.

Elastic-plastic stress analysis is performed for each simulated corrosion layer removed. The analyses are performed using ANSYS [2] and described in the next section.

4.0 ANALYSIS

There are two groups of analyses described in this section: (1) residual stress analysis due to solution anneal and quenching, and (2) residual stress analysis for each corrosion layer removed, which simulates loss of material loss due to general corrosion.

4.1 Residual Stress Analysis Due to Solution Anneal and Quenching

Three residual stress analyses are performed on the 20 *mm*-thick MWP model: (1) quench on the outside surface only (outside quench) using the BISO curves, (2) quench on both the inside and outside surfaces (double-sided quench) using the BISO curves, and (3) double-sided quench using the BKIN curves. Stress results at the end of quenching are compared to evaluate the difference between the three quenching processes. The analyses are performed using ANSYS [2] and the input files are described in Appendix A. All electronic input and output files are included with this calculation package.

These analyses determine the residual stresses caused by annealing and quenching on the MWP container outer shell. They follow the same techniques employed in Reference 1 using the same time steps, which are: two seconds from 45 to 285 seconds, five seconds from 285 to 600 seconds, and 10 seconds from 600 to 1801 seconds in the transient. It is assumed that any existing weld residual stress becomes negligible due to annealing, that is, the initial weld residual stress is eliminated by the annealing and replaced by the residual stress field dictated solely by quenching.

The simulated thermal cycle for the transient is identical to that in Reference 1: start with a uniform temperature of 1120°C and hold for 45 seconds, and then lower the outside surface temperature to a room temperature of 20°C in 1801 seconds to simulate the effect of quenching. The outside temperature history is presented in Figures 3 through 5 (annotated as OD temperature) for the three analyses described in the first paragraph of this section.

4.2 Residual Stress Analysis for Effect of General Corrosion

Section 4.1 provided a description of the analysis to obtain the residual stress field caused by the annealing and quenching. After the quench, the model is then subjected to a steady state room temperature of 20°C, and followed by another steady state operating temperature of 125°C. Note that the 125°C is not associated with the quenching process but rather with the operating temperature.

This residual stress is the stress state at the beginning of service for the waste package container outer shell. However, due to general corrosion that can occur, material that is subjected to compressive stress at the beginning of service will corrode away. Loss of this material will cause the residual stress to redistribute since force and moment equilibrium must exist across the cross-section of the wall. Thus, an analysis is required to determine the redistribution of residual stress with time as general corrosion occurs.

This analysis resumes from the end of the residual stress analysis (final steady state at operating temperature of 125°C) and determines the effect of corrosion by removing one outer layer at a time. The analysis is performed at 125°C operating temperature, which is a reasonable upper bound temperature for corrosion to occur in the repository. A total of four layers are removed, resulting in removal of 40% of the middle section thickness (see Figure 1). Through-wall axial and hoop stresses for Sections 1 to 4 defined in Figure 1 are then extracted. Axial stress acts on a circumferential flaw and hoop stress acts on an axial flaw (a flaw that grows radially into the MWP wall and the crack plane is parallel to the MWP longitudinal axis). The removal of the layers is simulated using the element life and death capabilities of ANSYS [2].

4.3 Stress Intensity Factor Calculation

Stress intensity factors (K) are calculated for the residual stress on the refined model at 125°C for the remaining ligament after each layer is removed. The calculation is performed using pc-CRACK [4] and the **Linear-Elastic Fracture Mechanics** (LEFM) approach. For sections 2 and 3 under axial stress (SY), a **Single Edge Cracked Plate** (SECP) model is used. For the sections under hoop stress (SZ), an **Elliptical Surface Crack in an Infinite Plate (a/l = 0.5)** model is used. Based on experience, this a/l is a reasonable value to use. The stress intensity factor will vary if the a/l is changed. However, the intention of this evaluation is to better understand the behavior of the residual stress. And, different crack aspect ratios will change the magnitude of the driving force on the crack, but will not change the nature of the driving force, whether it is tensile or compressive. Therefore, a/l is not a critical factor and the use of one a/l ratio consistently throughout the evaluation will yield consistent results for comparison. The maximum depth of the cracks is 80% through-wall from the outside surface since the LEFM validity is violated for deeper flaws. Different LEFM models are selected because a circumferential flaw is subjected to axial stress around the circumference of the MWP, while an axial flaw is subjected to hoop stress around the circumference of the MWP.

5.0 RESULTS OF ANALYSIS AND DISCUSSIONS

The results of the analyses described in Section 4.0 are provided in this section. The results presented focus on the stress profiles for Sections 1 to 4 representing a general trend at various sections of the MWP container outer shell.

5.1 Stress Results Due to Annealing and Quenching

Figures 3 through 5 present the temperature history on locations near the top, middle, and bottom portions of the inside surface, as well as on the outside surface. The temperature curves for the outside and inside quench analyses using the BISO curves (Figure 4) and the BIKN curves (Figure 5) are identical. This implies that the usage of different isotropic hardening curves do not affect the thermal transient response of the model. Figures 6 through 8 shows the exaggerated deformed shapes for the three analyses at the end of quenching (time = 1801 sec.). Detailed discussions on the stress distributions are discussed below.

Figures 9 through 14 plot the overall radial (SX), axial (SY), and hoop (SZ) stress distributions at 125°C operating temperature (time = 1803 sec.), for the analyses using the BISO curves. The results show that, when using the same material curves, double-sided quenching results in more compressive stresses on the outside surface than quenching on the outside surface only. The figures also show that Section 4 cuts through the maximum tensile axial stress regions on the inside surface.

The stress profiles at 125°C operating temperature for Sections 1 to 4 are extracted, processed in Excel workbook POST319.XLS, and plotted in Figures 15 through 18 for analyses using the BISO curves, and Figures 19 through 22 for the double-sided quenching analyses using different material curves. The results confirm that double-sided quenching results in more compressive stresses on the outside surface of the MWP outer shell (comparing Figures 15 through 18), especially in the section where there is tensile on the outside surface due to outside quench only (see Figure 17). And, while the resultant stresses for the BISO and BKIN curves are similar, the results using the BKIN curves result in lower stresses (i.e., less compressive and less tensile stresses) than that using the BISO curves (comparing Figures 19 through 22).

In addition, the outside surface stress plots at an operating temperature of 125°C shown in Figures 23 and 24 on the side wall of the MWP also demonstrate that the double-sided quench analyses do result in more compressive stress on the outside surface of the MWP outer shell, while the double-sided quench analysis using the BKIN curves results in less compressive stresses than that using the BISO curves. Therefore, the analysis using the BKIN curves is the bounding case.

Another observation from the resultant stress plots shows that the radial stress (SX) has negligible contribution to the overall behavior of the model. Therefore, the radial stress is not considered in the corrosion analysis.

5.2 Stress Results Due to General Corrosion

The results for the three corrosion analyses using different bilinear hardening curves for the material and quenching processes are reported separately below. The corrosion analysis is performed at a steady-state operating temperature of 125°C.

5.2.1 Results for outside quench analysis using BISO curves

Representative axial and hoop stress distributions at 125°C operating temperature and due to general corrosion on the model are shown in Figures 25 through 30 for the outside quench analysis using the BISO curves. The radial stress is not considered since it is insignificant and it only acts on a subsurface planner flaw.

The sectional stress results are also processed in POST319.XLS. The through-wall axial and hoop stresses, in global Cartesian coordinates, for Sections 1 to 4 are plotted in Figures 31 through 38. The numbered labels for the curves denote the thickness of the corrosion in millimeters (*mm*) from the outside surface.

The plots in Figures 31, 32, and 34 show the general trend of through-wall axial stresses for Sections 1, 2, and 4, respectively; the results show negative axial stresses on the outside surface even after 40% of the wall thickness is removed. But for Section 3, the axial stress on the outside surface remains positive (see Figure 33). Note that for Section 1, the stress redistribution is smaller than that for Sections 2, 3, and 4. This is due to the fact that the wall thickness for Section 1 is much greater than that for the other sections. The expected behavior of the stress redistribution is very complicated since it is due to many parameters such as wall thickness, shape of the residual stress profile, three-dimensional stress state of discontinuity stress, and relaxation.

The plots in Figures 35 through 38 also show a general trend of decreasing through-wall hoop stresses for decreasing thickness for Sections 1, 2, 3, and 4, respectively. As mentioned earlier, the redistribution of the stress is extremely complex since it is due to many parameters. However, for all sections on the outer surface, the hoop stress remains compressive after 40% of the wall material is removed.

5.2.2 Results for double-sided quench analysis using BISO curves

The sectional stress results for the double-sided quench analysis using the BISO curves are processed in POST319.XLS. The through-wall axial and hoop stresses at 125°C operating temperature, in global Cartesian coordinates, for Sections 1 to 4 are plotted in Figures 39 through 46. The numbered labels for the curves denote the thickness of the corrosion in millimeters (*mm*) from the outside surface.

The plots in Figures 39 and 42 show the general trend of through-wall axial stresses for Sections 1 and 4, respectively. The results show negative axial stresses on the outside surface even after 40% of the wall thickness is removed. But for Sections 2 and 3, the axial stresses on the outside surface becomes

positive (see Figures 40 and 41). As mentioned in the previous section, the redistribution of the stress is extremely complex since it is due to many parameters.

The plots in Figures 43 through 46 show the general trend of the hoop stresses for Sections 1, 2, 3, and 4, respectively. It can be seen from the plots that the hoop stresses on the outsider surface for Sections 1 and 4 remains negative when 40% of the wall thickness is removed (Figures 43 and 46), but for Sections 2 and 3, the hoop stresses on the outside surface become more positive when more wall material is removed (Figures 44 and 45).

5.2.3 Results for double-sided quench analysis using BKIN curves

The sectional stress results for the double-sided quench analysis using the BKIN curves are processed in POST319.XLS. The through-wall axial and hoop stresses at 125°C operating temperature, in global Cartesian coordinates, for Sections 1 to 4 are plotted in Figures 47 through 54. The numbered labels for the curves denote the thickness of the corrosion in millimeters (*mm*) from the outside surface.

The plots in Figures 47 through 50 show the general trend of through-wall axial stresses for Sections 1 through 4, respectively. The results show very similar trends to the double-sided quench analysis using the BISO curves: The axial stresses on the outside surface for Sections 1 and 4 are negative even after 40% of the wall thickness is removed (Figures 47 and 50). But for Sections 2 and 3, the axial stresses on the outside surface remains positive (see Figures 48 and 49). As mentioned in the previous section, the redistribution of the stress is extremely complex since it is due to many parameters.

The plots in Figures 51 through 54 show the general trend of the hoop stresses for decreasing thickness for Sections 1 through 4, respectively. It can be seen from the plots that the results show very similar trends to the double-sided quench analysis using the BISO curves: the hoop stresses on the outsider surface for Sections 1 and 4 remains negative when 40% of the wall thickness is removed (Figures 51 and 54), but for Sections 2 and 3, the hoop stresses on the outside surface become more positive when more wall material is removed (Figures 52 and 53).

5.3 Results for Stress Intensity Factors

The stress intensity factor results for the three corrosion analyses are discussed separately below.

5.3.1 Results for outside quench analysis using BISO curves

The stress intensity factors (K) for the model due to axial and hoop stresses for Sections 2 and 3 with varying thickness are calculated using pc-CRACK [4]. Only Sections 2 and 3 are considered because they represent the thinnest portion of the MWP wall. The pc-CRACK outputs are then imported, processed, and plotted using Excel in spreadsheet POST319.XLS. The stress intensity factors are plotted in Figures 55 through 58. The curves show the stress intensity factors due to the axial and hoop stresses vs. normalized crack depth (a/t) for Sections 2 and 3. The numbered labels for the curves denote the thickness of the corrosion in millimeters (*mm*).

The stress intensity factor plots show that, except for a circumferential crack at Section 3 due to axial stress (Figure 56), the Ks for the uncorroded and corroded MWP initialize negatively so that cracking is unlikely to occur and propagate (Figures 55, 57, and 58). As for the case of the circumferential crack at Section 3 driven by axial stress, the Ks for the uncorroded and corroded MWP go more positively as depth increases indicating that a circumferential flaw at Section 3 is likely to grow (see Figure 56).

5.3.2 Results for double-sided quench analysis using BISO curves

The stress intensity factors (K) for the refined model due to axial and hoop stresses for Sections 2 and 3 with varying thickness are calculated using pc-CRACK [4]. Only Sections 2 and 3 are considered because they represent the thinnest portion of the MWP wall. The pc-CRACK outputs are then imported, processed, and plotted using Excel in spreadsheet POST319.XLS. The stress intensity factors are plotted in Figures 59 through 62. The curves show the stress intensity factors due to the axial and hoop stresses vs. normalized crack depth (a/t) for Sections 2 and 3. The numbered labels for the curves denote the thickness of the corrosion in millimeters (*mm*).

The plots show that the stress intensity factors increase with decreasing thickness for all sections. Therefore, a circumferential or an axial flaw at any of these locations is likely to grow.

5.3.3 Results for double-sided quench analysis using BKIN curves

The stress intensity factors (K) for the refined model due to axial and hoop stresses for Sections 2 and 3 with varying thickness are calculated using pc-CRACK [4]. Only Sections 2 and 3 are considered because they represent the thinnest portion of the MWP wall. The pc-CRACK outputs are then imported, processed, and plotted using Excel in spreadsheet POST319.XLS. The stress intensity factors are plotted in Figures 63 through 66. The curves show the stress intensity factors due to the axial and hoop stresses vs. normalized crack depth (a/t) for Sections 2 and 3. The numbered labels for the curves denote the thickness of the corrosion in millimeters (*mm*).

The plots show very similar trends to the double-sided quench analysis using the BISO curves: that the stress intensity factors increase with decreasing thickness for all sections. Therefore, a circumferential or an axial flaw at any of these locations is likely to grow.

6.0 CONCLUSIONS

Residual stress analyses are performed on the outside surface only quenching and inside and outside surface quenching for the 20 *mm*-thick 21 PWR Mockup Waste Package container outer shell. Comparing the stress results conclude that quenching on both the inside and outside surfaces will bring compressive residual stresses on the outside surface of the MWP at an operating temperature of 125°C.

The general trend on residual stresses at selected locations of the model is evaluated for the effect of general corrosion on the outside surface of the container outer shell. Results show that corrosion has no significant adverse effect on the outside surface quenching, but it would reduce the compressive stress for the double-sided quenching.

Comparing the results between bilinear isotropic hardening and bilinear kinematic hardening properties concluded that the usage of bilinear kinematic would yield more conservative results.

In addition, calculation on the stress intensity factors for the model utilizing outside surface quenching shows that negative intensity factors exist through most of the wall thickness where there is compressive residual stress on the outside surface of the container outer shell. For sections with tensile residual stress on the outside surface, the stress intensity factor is always positive through the wall thickness. Therefore, if a crack is initiated at this location, the residual stress would provide driving force for the stress corrosion crack growth through the remaining wall thickness.

Calculation on the stress intensity factors for the model utilizing double-sided quenching demonstrates that the stress intensity factors are mostly positive at the selected locations. Therefore a crack is likely to initiate at this location, and the residual stress would provide driving force for the stress corrosion crack growth through the remaining wall thickness.

7.0 REFERENCES

1. SI Calculation Package TRW-06Q-318, Rev. 1, "Residual Stress Analyses on the 21 PWR Mockup Waste Package Outer Shell Due to Quenching and General Corrosion Using a Side-wall Thickness of 25 mm."
2. ANSYS/Mechanical, Revision 5.7, ANSYS Inc., December 2000.
3. [Not Used]
4. pc-CRACK for Windows, Version 3.1-98348, Structural Integrity Associates, Inc., December 1998.

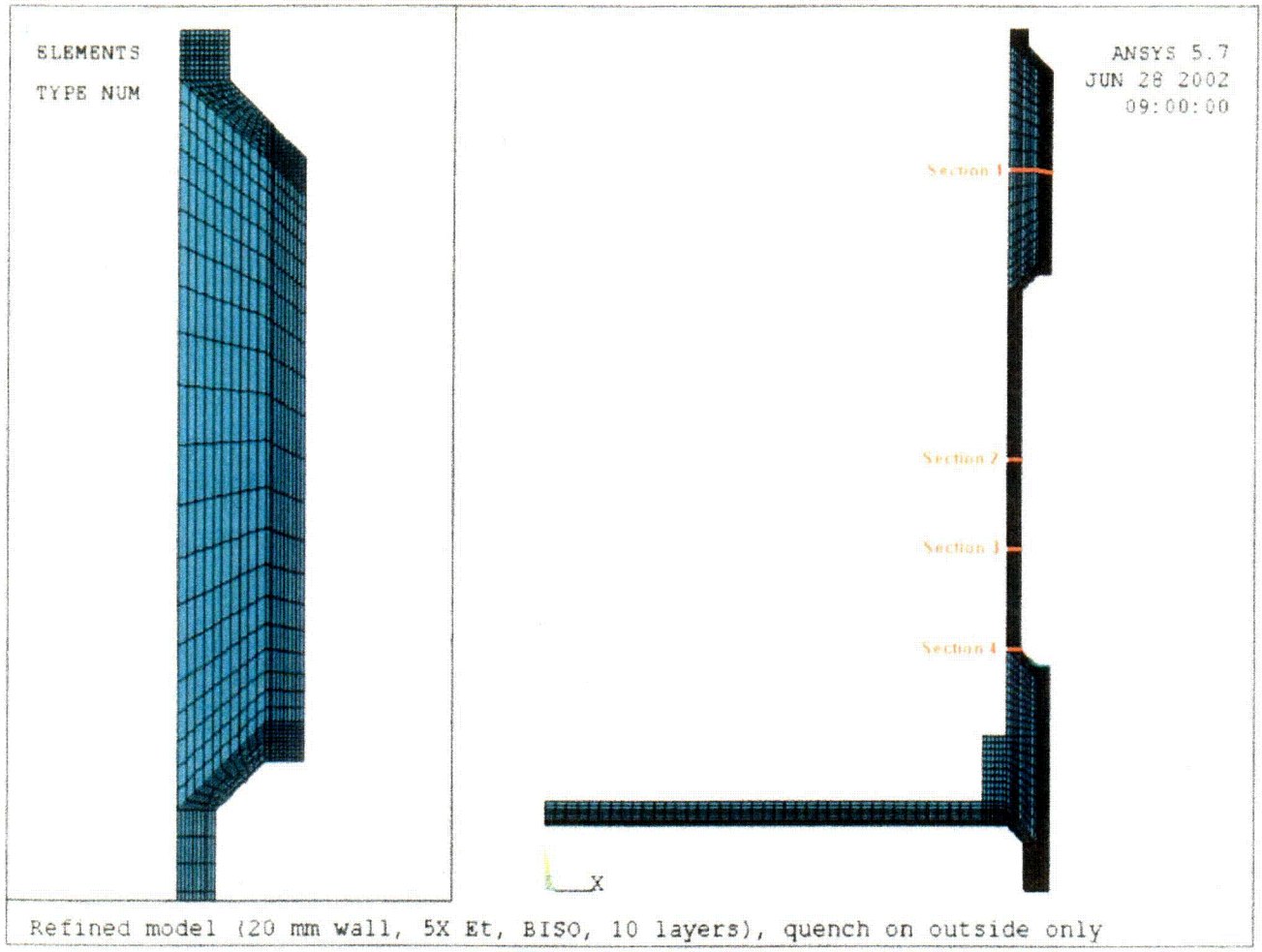

Figure 1: Finite Element Model with 20 mm-Thick Middle Wall

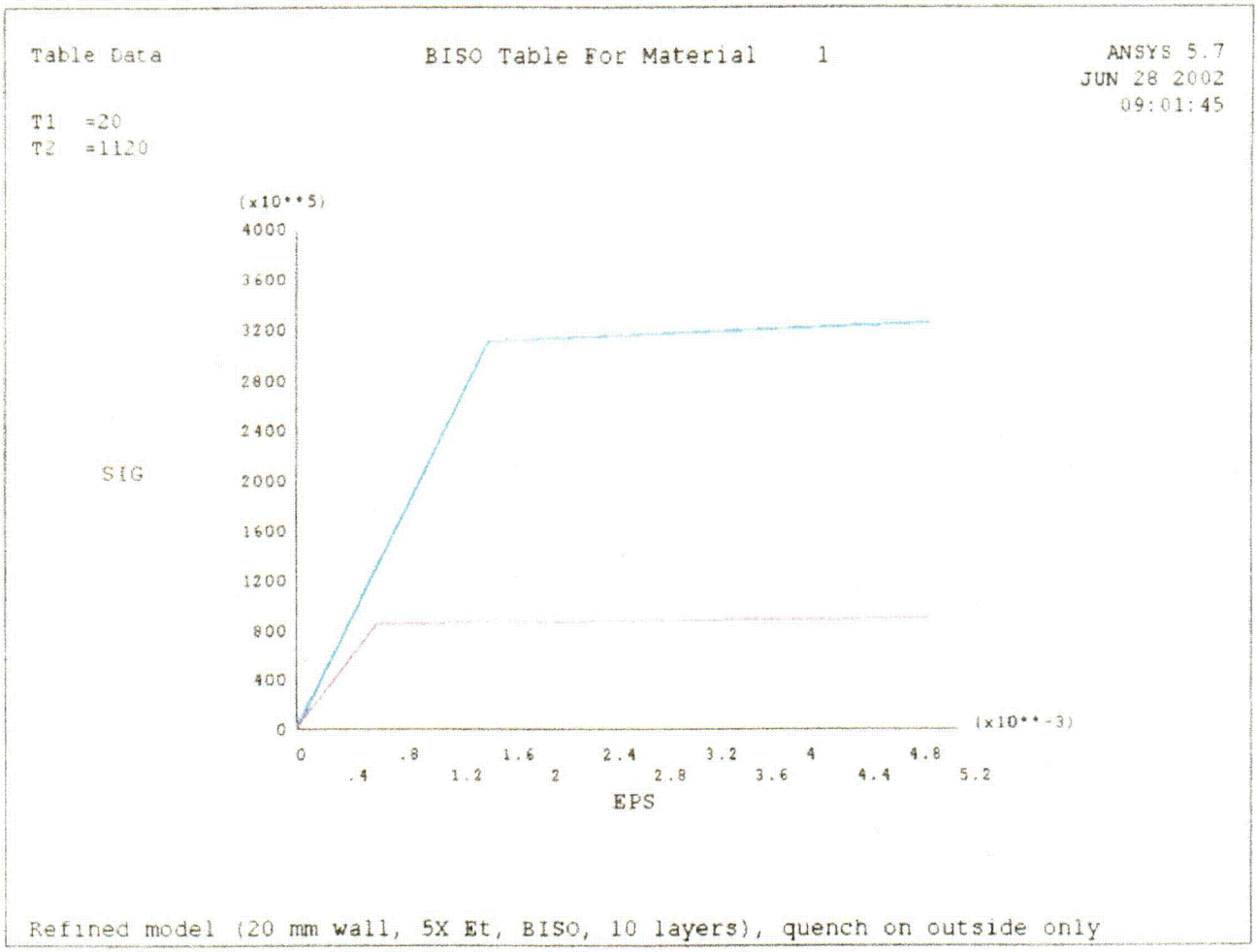

Figure 2: Adjusted Stress-Strain Curves for the Material

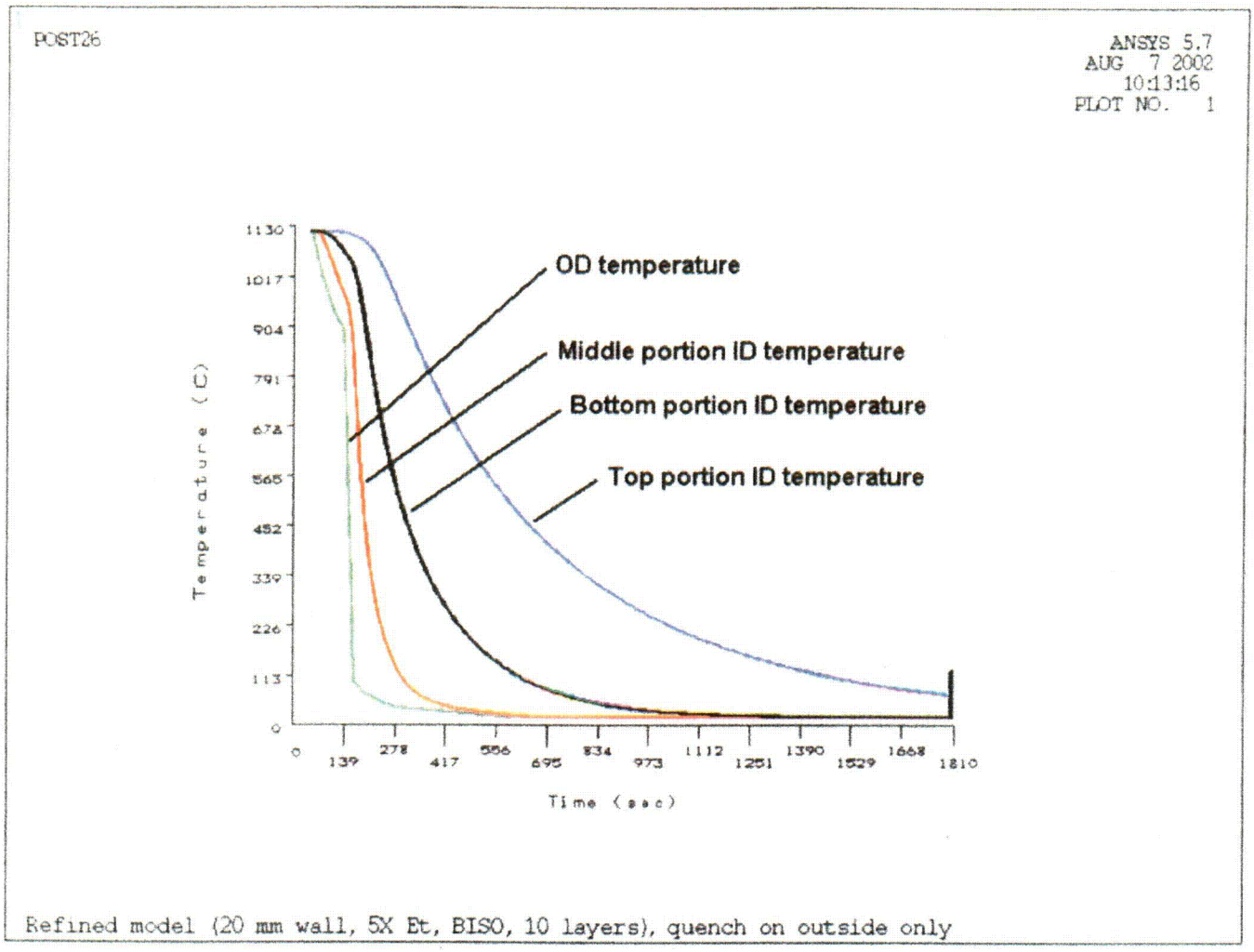

Figure 3: Temperature History at Various Locations of the Outside Quench Analysis Using the Bilinear Isotropic Hardening (BISO) Curves

OD – Outside surface (near the middle of the thin middle portion)
Top ID – Top inside surface (near the middle of the thick top portion)
Middle ID – Middle inside surface (near the middle of the thin middle portion)
Bottom ID – Bottom inside surface (near the middle of the thickest bottom portion)

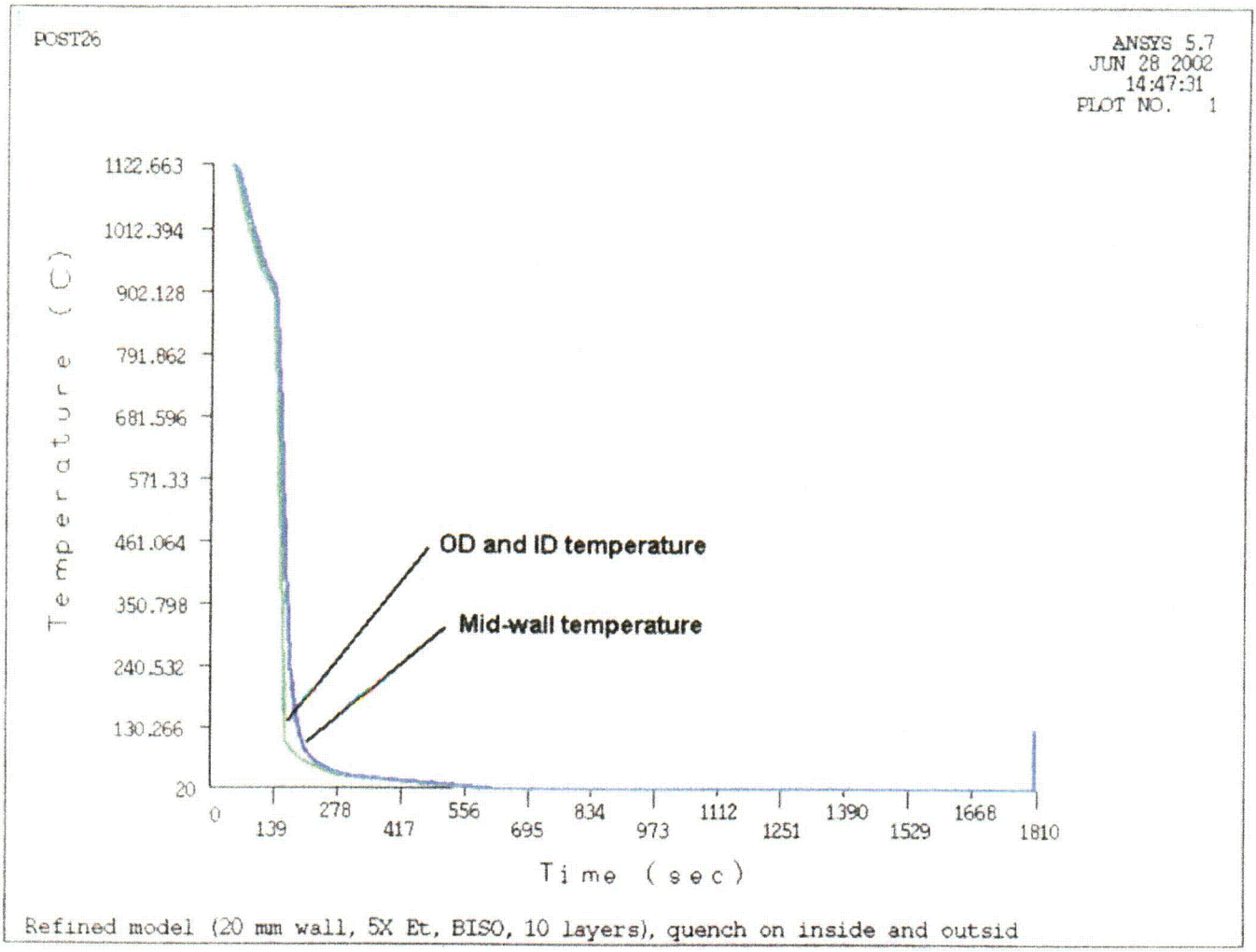

Figure 4: Temperature History of the Inside and Outside Quench Analysis Using the Bilinear Isotropic Hardening (BISO) Curves

OD and ID – Outside and inside surface (near the middle of the thin middle portion)
Mid-wall – Mid-point across the wall thickness (near the middle of the thin middle portion)

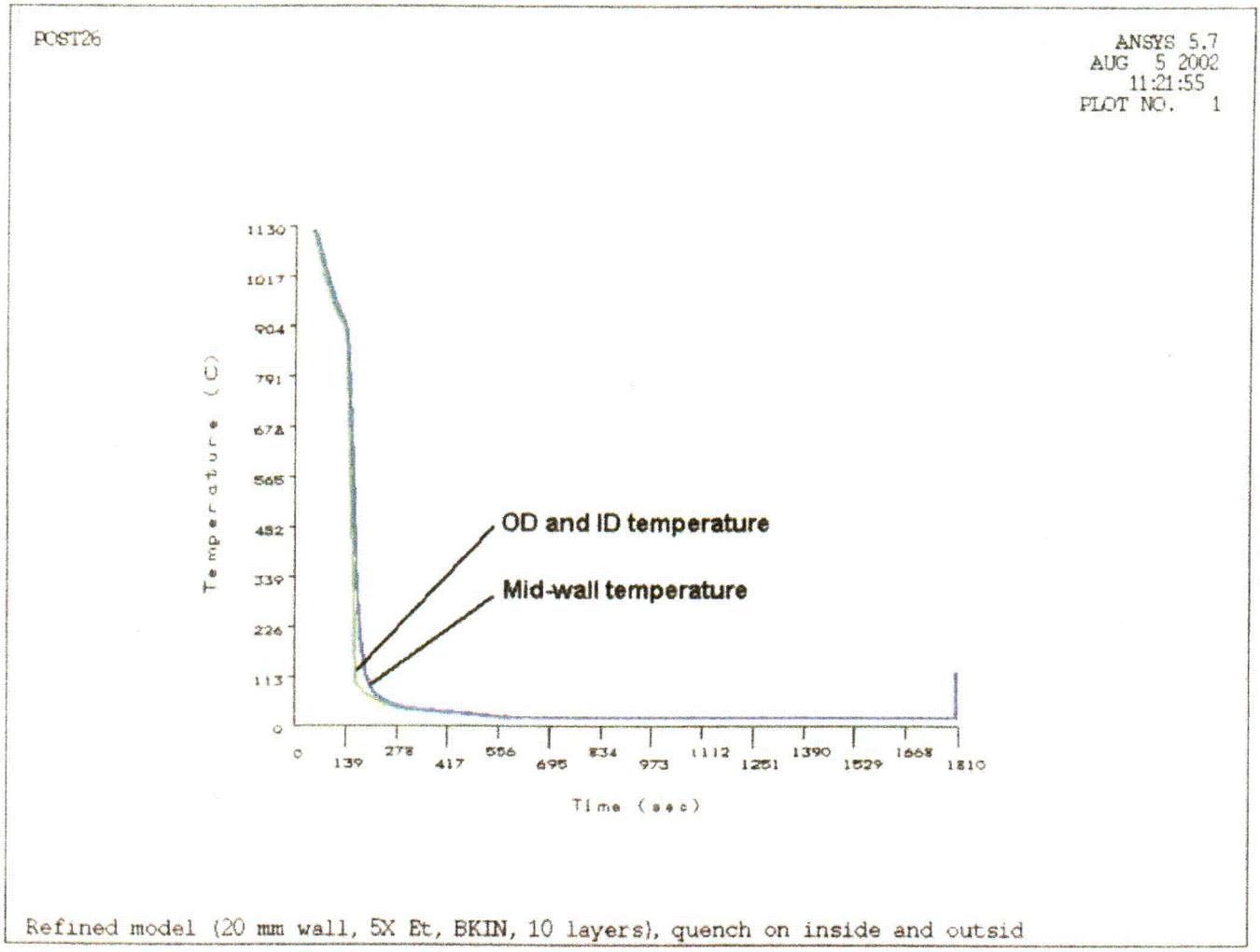

Figure 5: Temperature History of the Inside and Outside Quench Analysis Using the Bilinear Kinematic Hardening (BKIN) Curves

OD and ID – Outside and inside surface (near the middle of the thin middle portion)
Mid-wall – Mid-point across the wall thickness (near the middle of the thin middle portion)

Figure 6: Deformed Shapes at the End of Outside Quenching Using BISO Curves

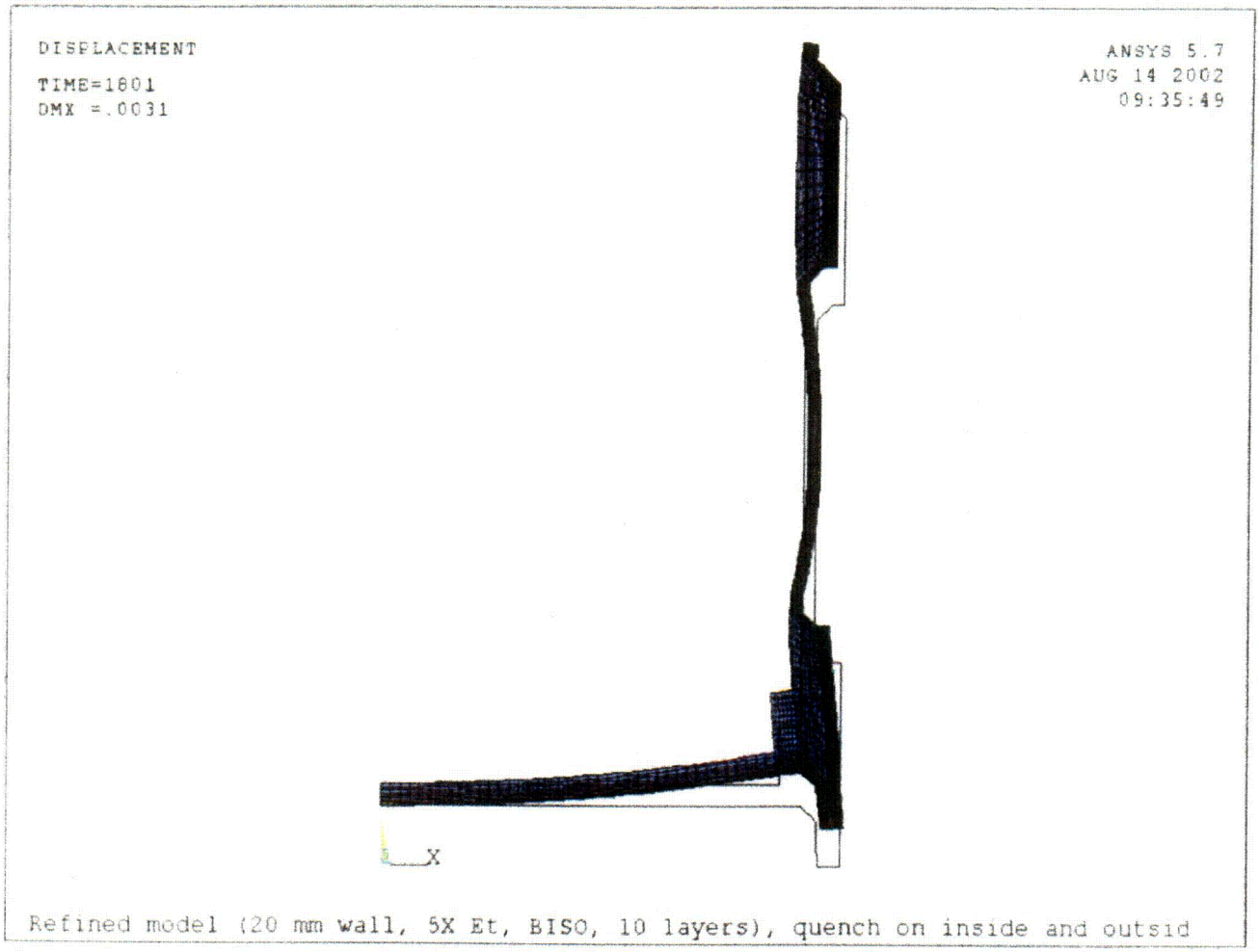

Figure 7: Deformed Shapes at the End of Double-Sided Quenching Using BISO Curves

Figure 8: Deformed Shapes at the End of Double-Sided Quenching Using BKIN Curves

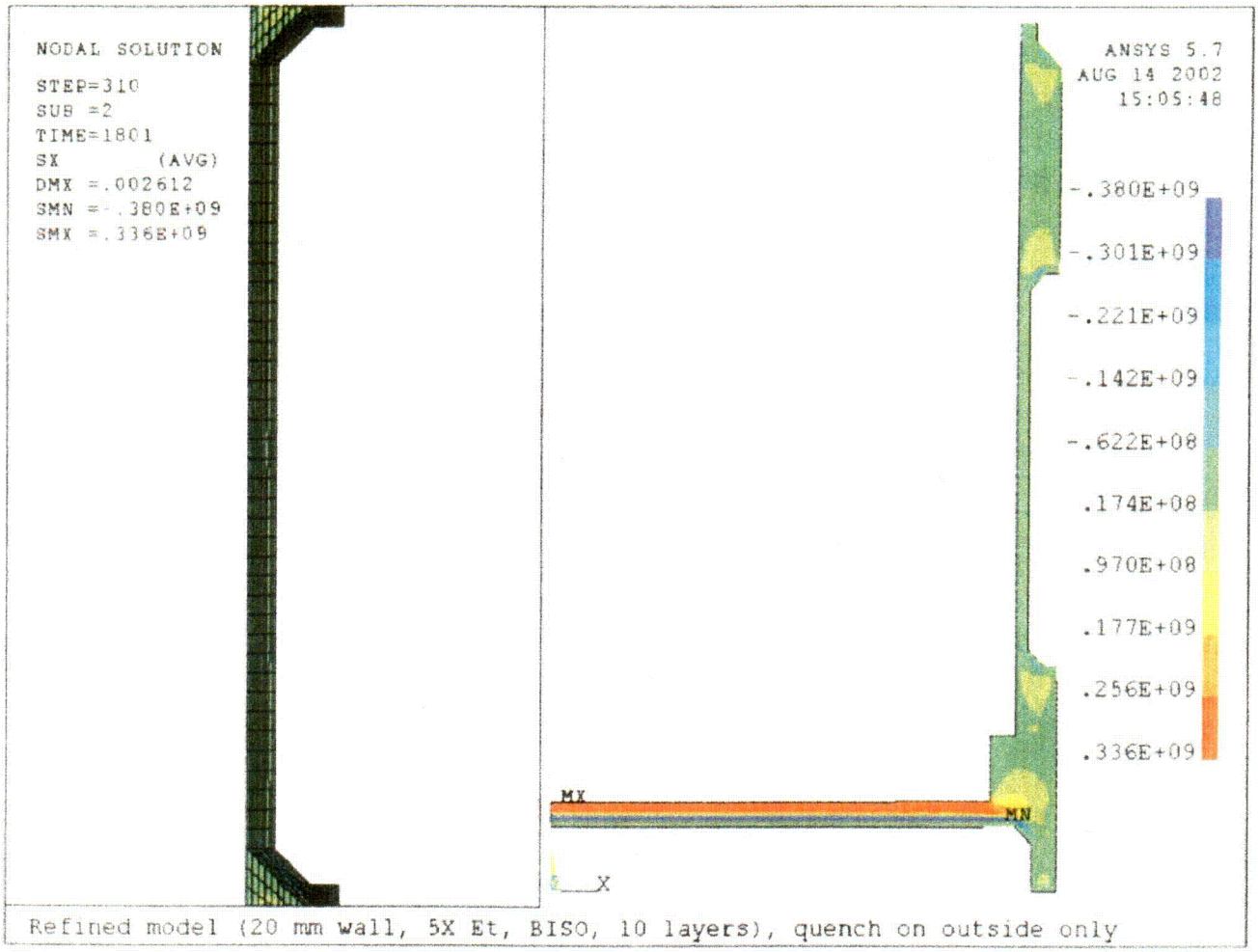

Figure 9: Radial Stress Plot for the Outside Quench Analysis Using BISO Curves at t = 1801 sec.

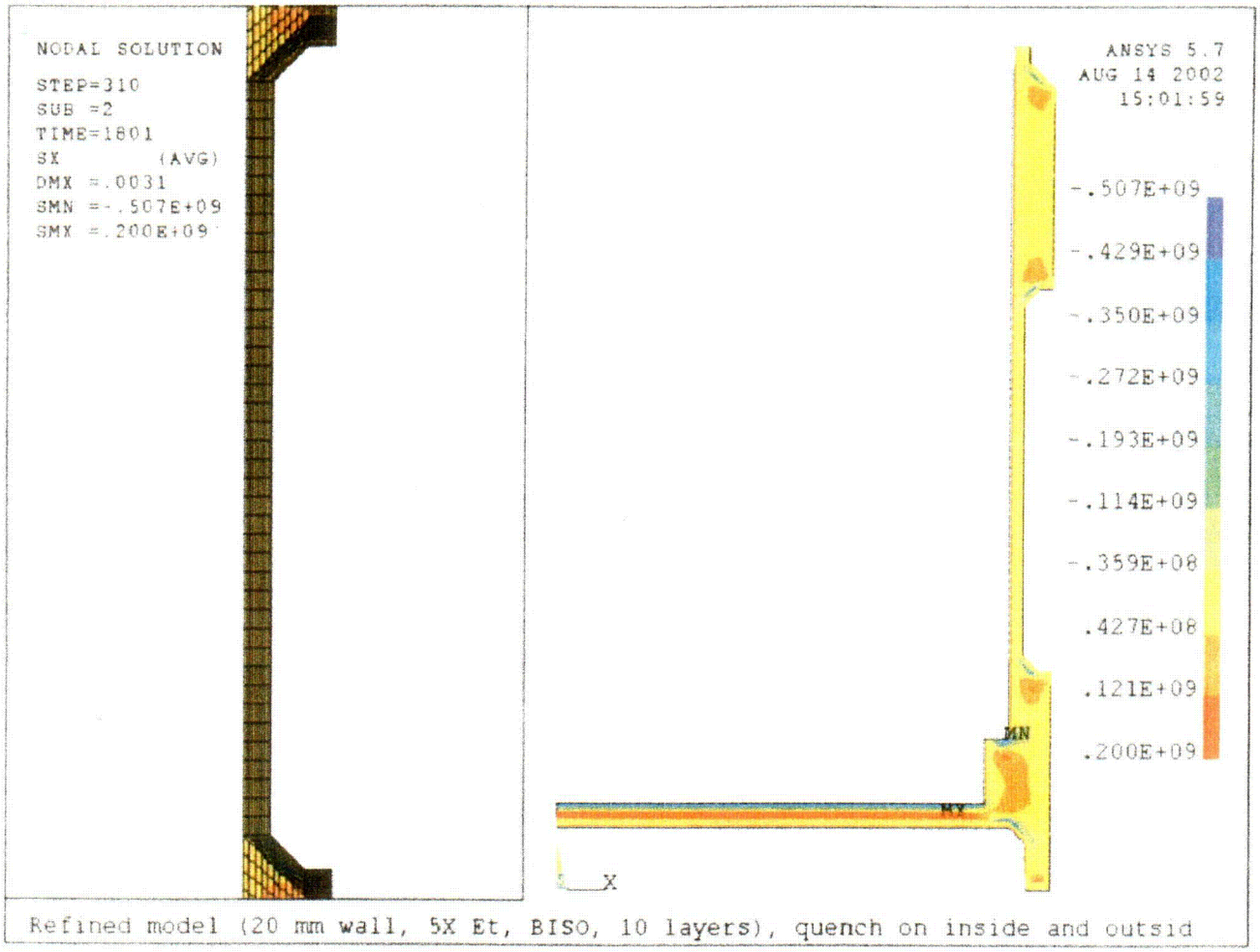

Figure 10: Radial Stress Plot for the Double-Sided Quench Analysis Using BISO Curves at t = 1801 sec.

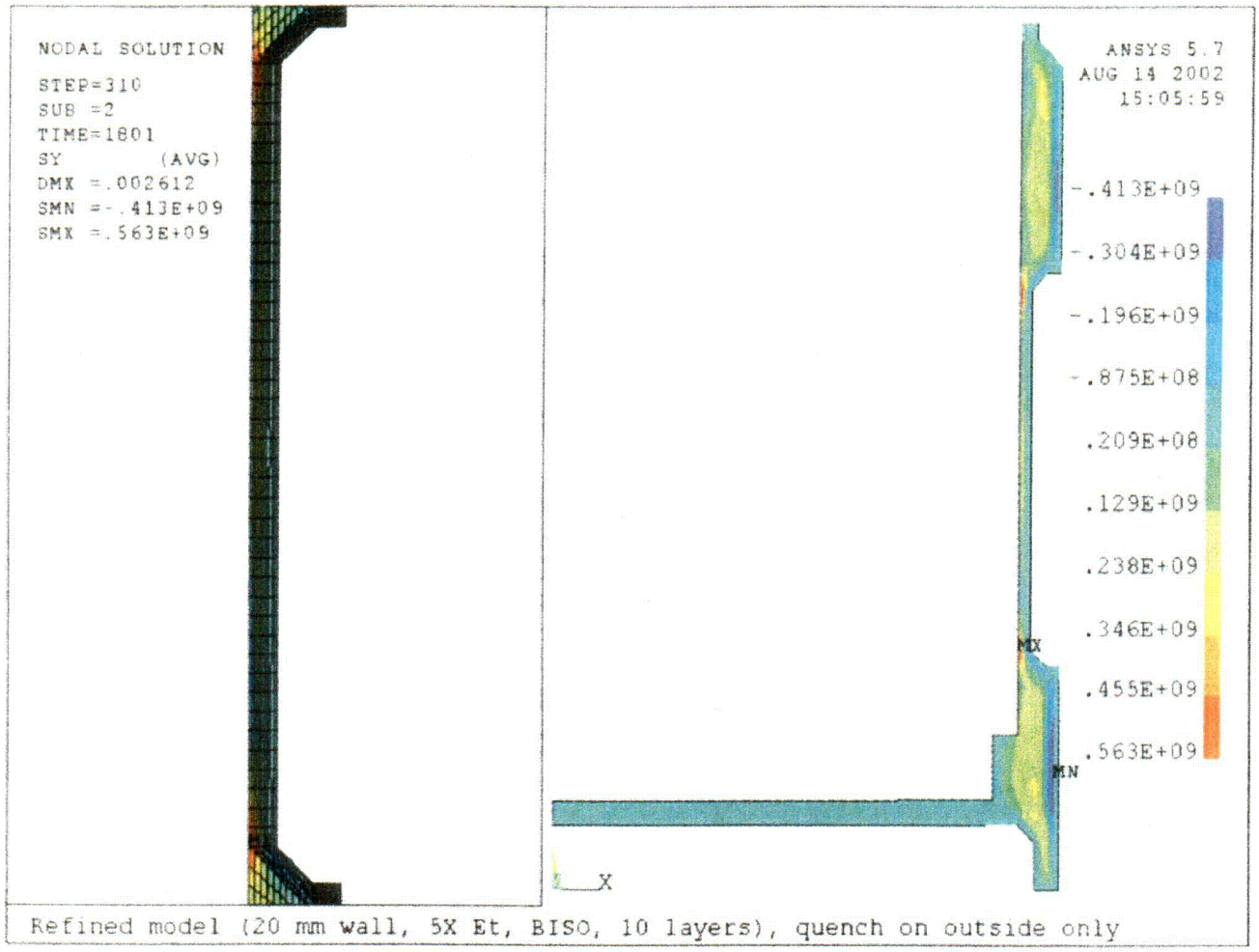

Figure 11: Axial Stress Plot for the Outside Quench Analysis Using BISO Curves at t = 1801 sec.

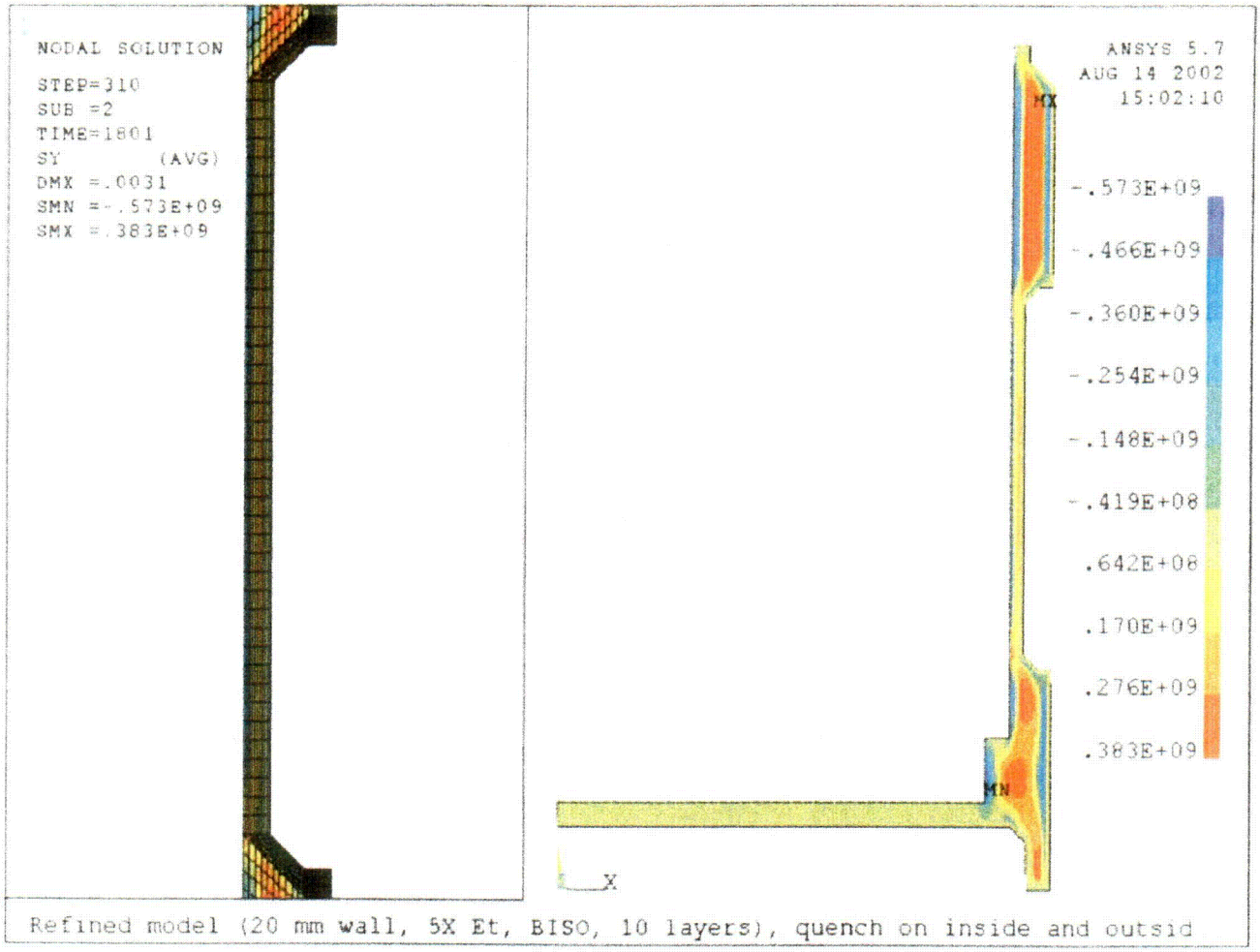

Figure 12: Axial Stress Plot for the Double-Sided Quench Analysis Using BISO Curves at t = 1801 sec.

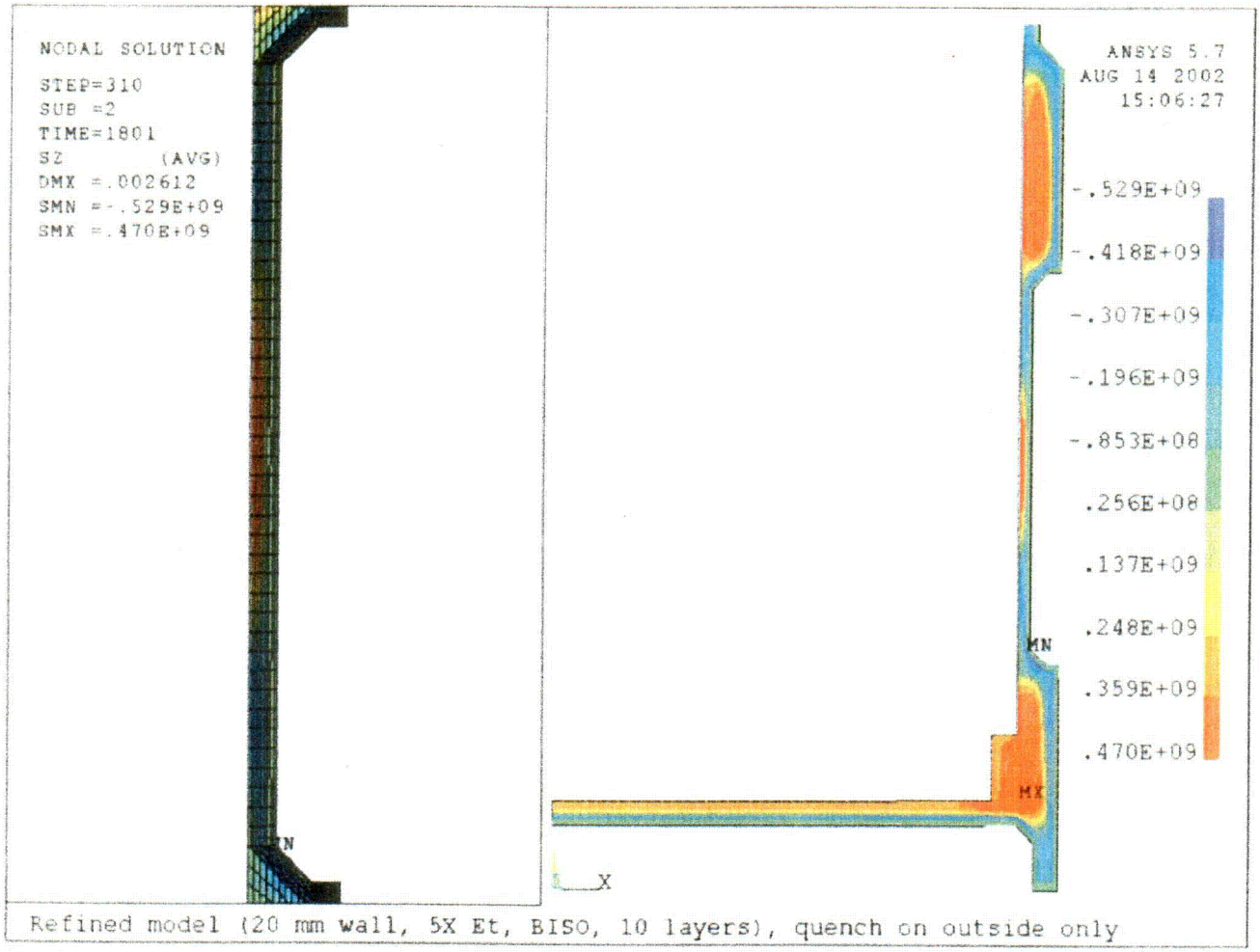

Figure 13: Hoop Stress Plot for the Outside Quench Analysis Using BISO Curves at t = 1801 sec.

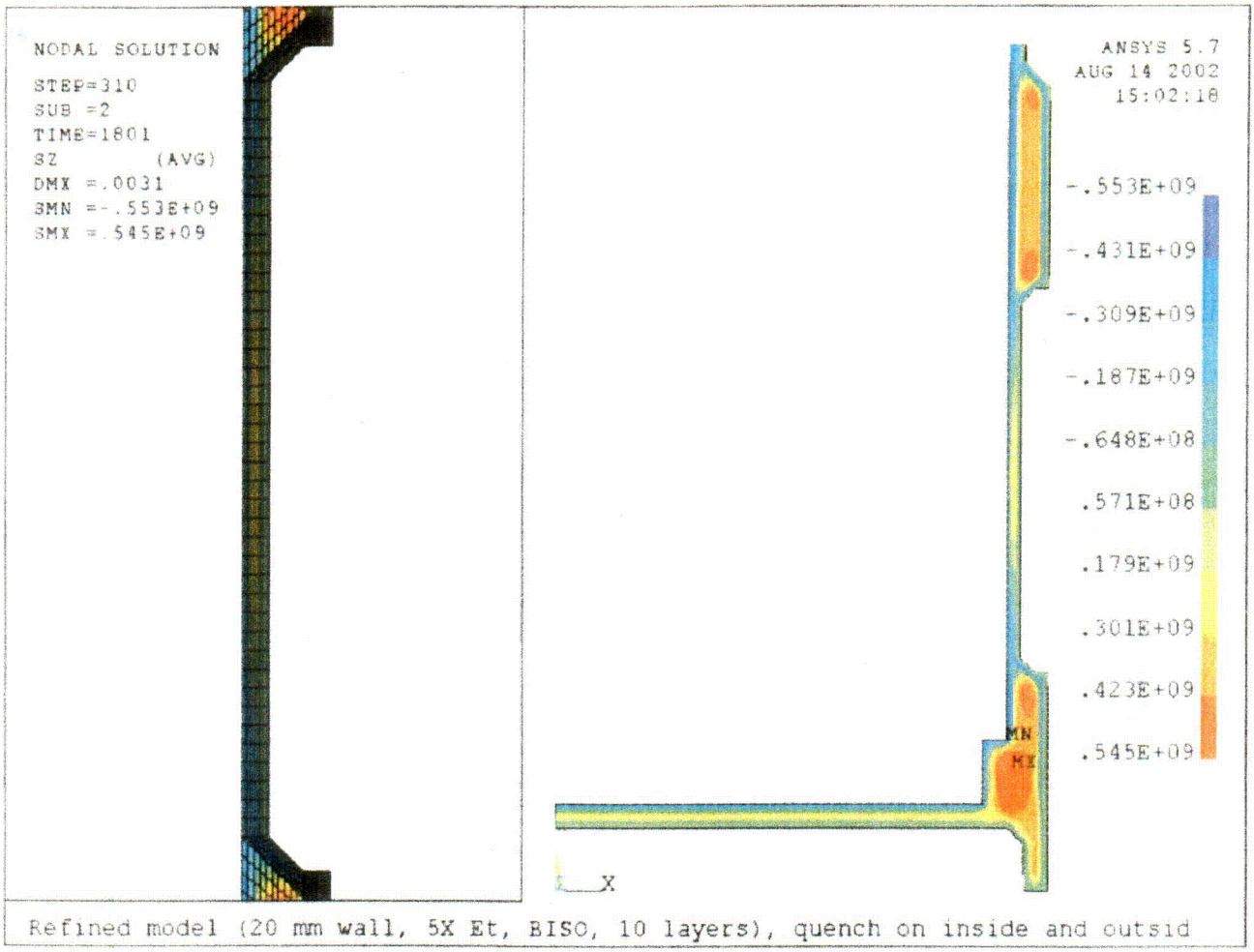

Figure 14: Hoop Stress Plot for the Double-Sided Quench Analysis Using BISO Curves at t = 1801 sec.

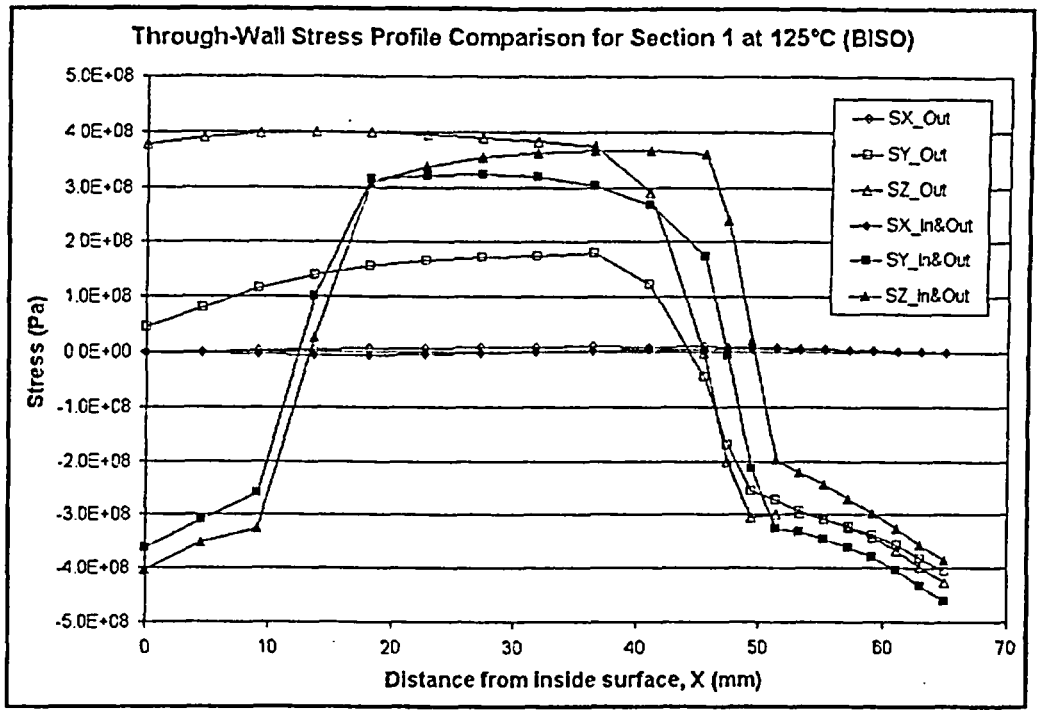

Figure 15: Stress Profile Comparison Between the Two Quenching Analyses Using BISO Curves, Section 1

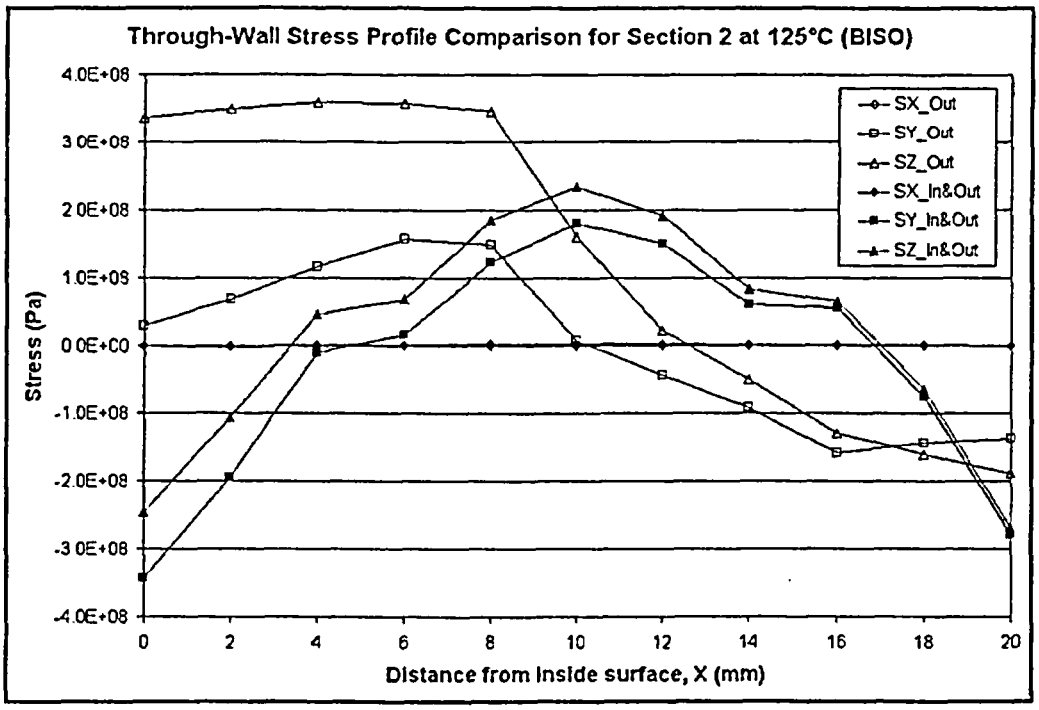

Figure 16: Stress Profile Comparison Between the Two Quenching Analyses Using BISO Curves, Section 2

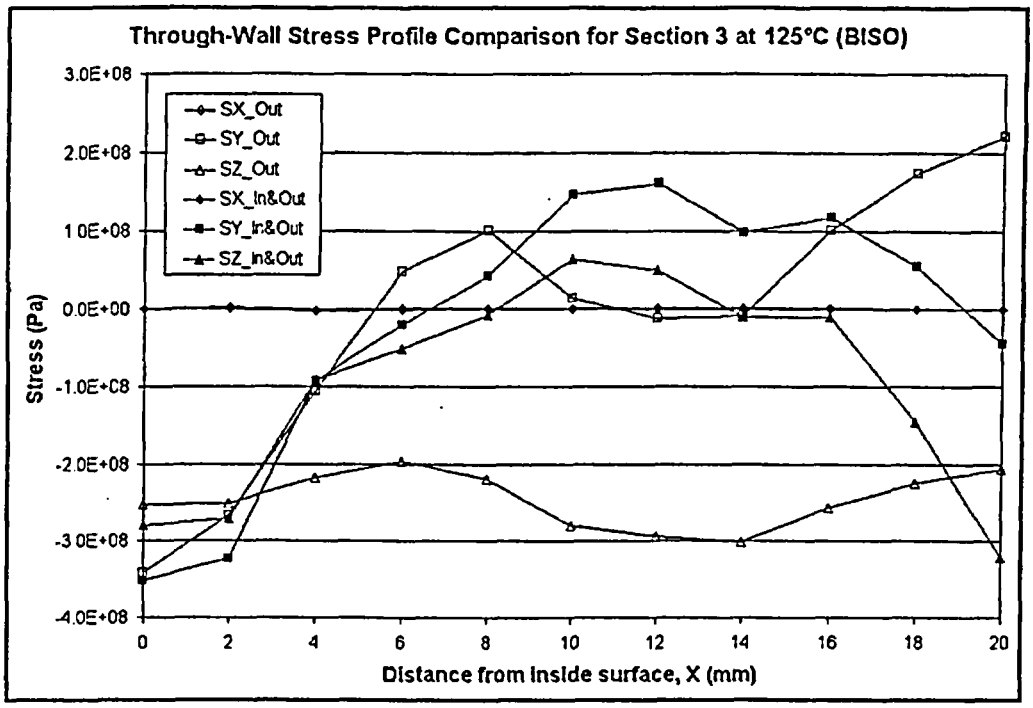

Figure 17: Stress Profile Comparison Between the Two Quenching Analyses Using BISO Curves, Section 3

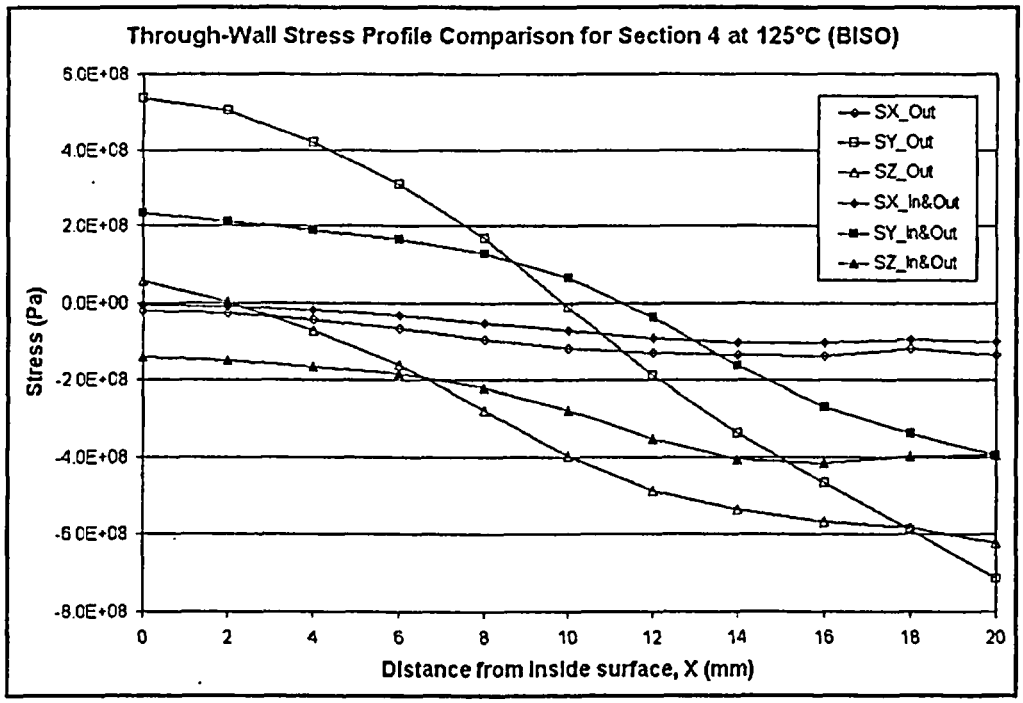

Figure 18: Stress Profile Comparison Between the Two Quenching Analyses Using BISO Curves, Section 4

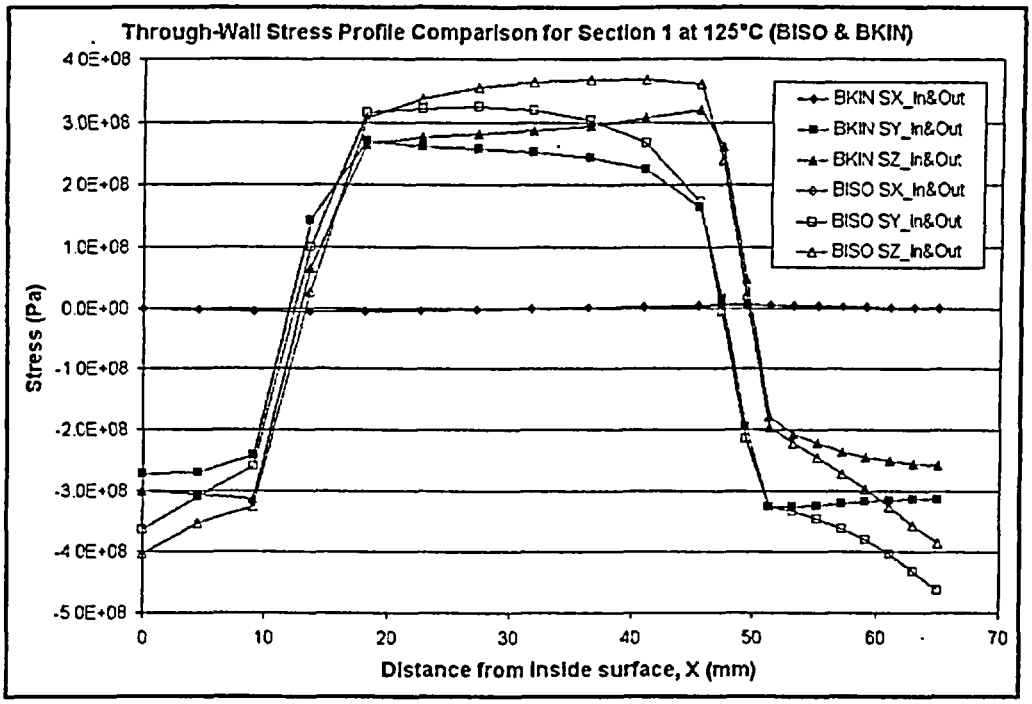

Figure 19: Stress Profile Comparison Between the Two Double-Sided Quenching Analyses, Section 1

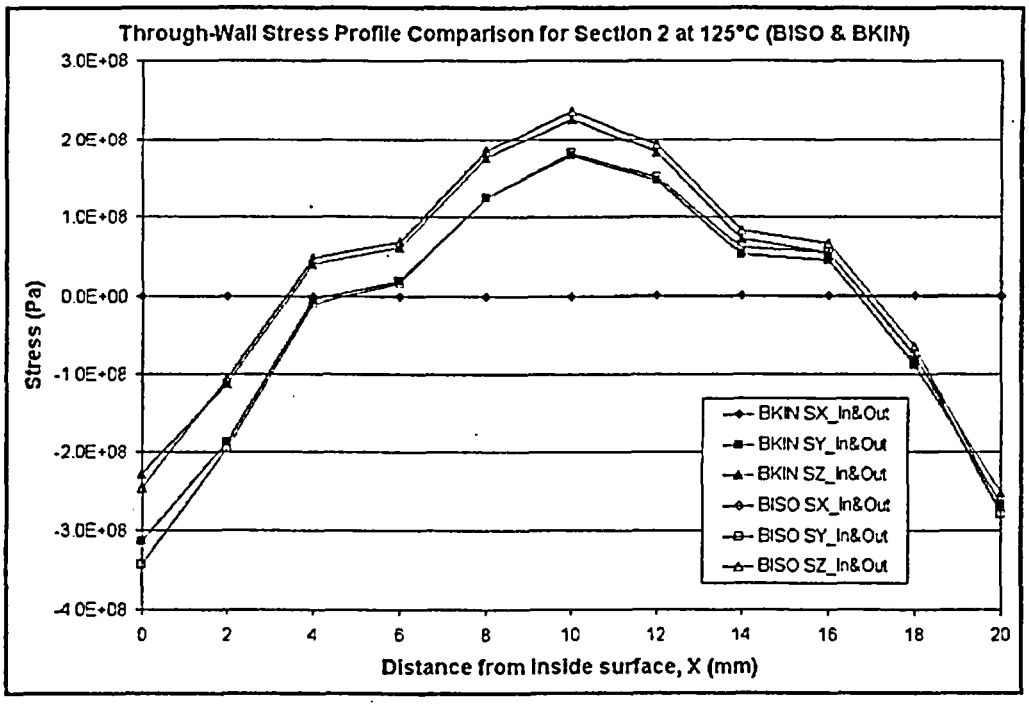

Figure 20: Stress Profile Comparison Between the Two Double-Sided Quenching Analyses, Section 2

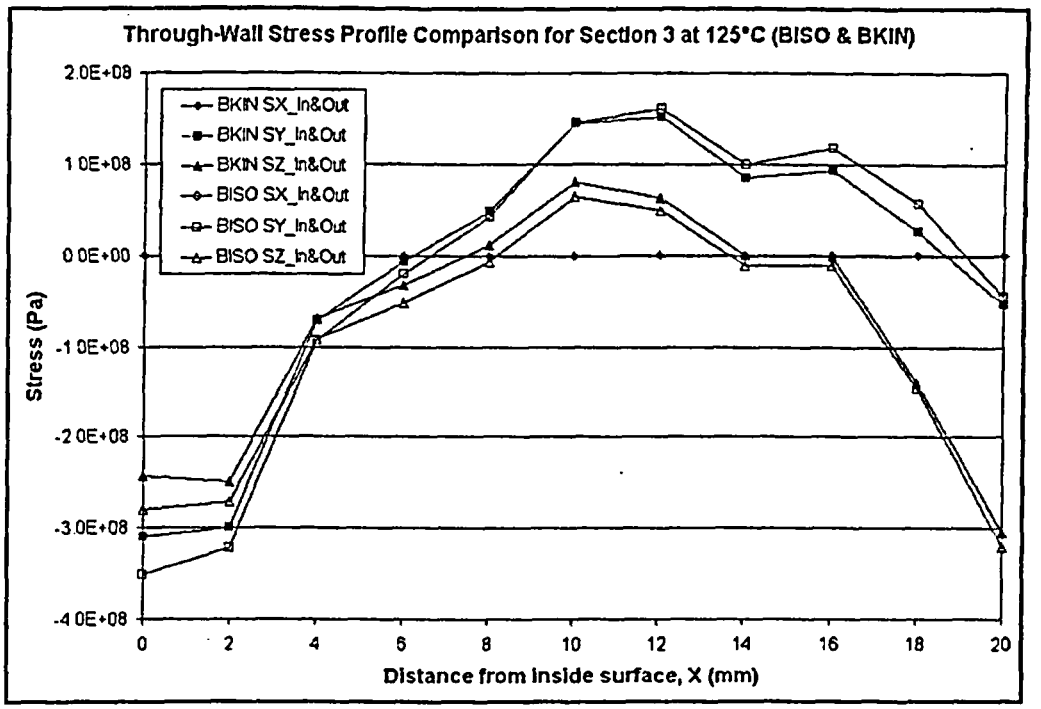

Figure 21: Stress Profile Comparison Between the Two Double-Sided Quenching Analyses, Section 3

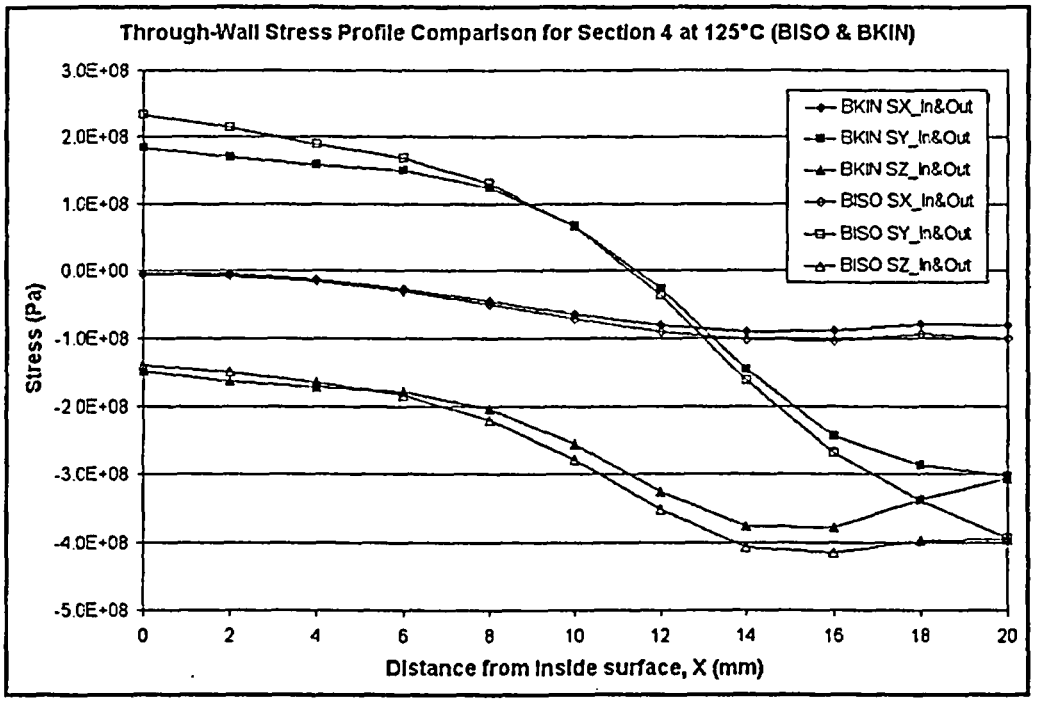

Figure 22: Stress Profile Comparison Between the Two Double-Sided Quenching Analyses, Section 4

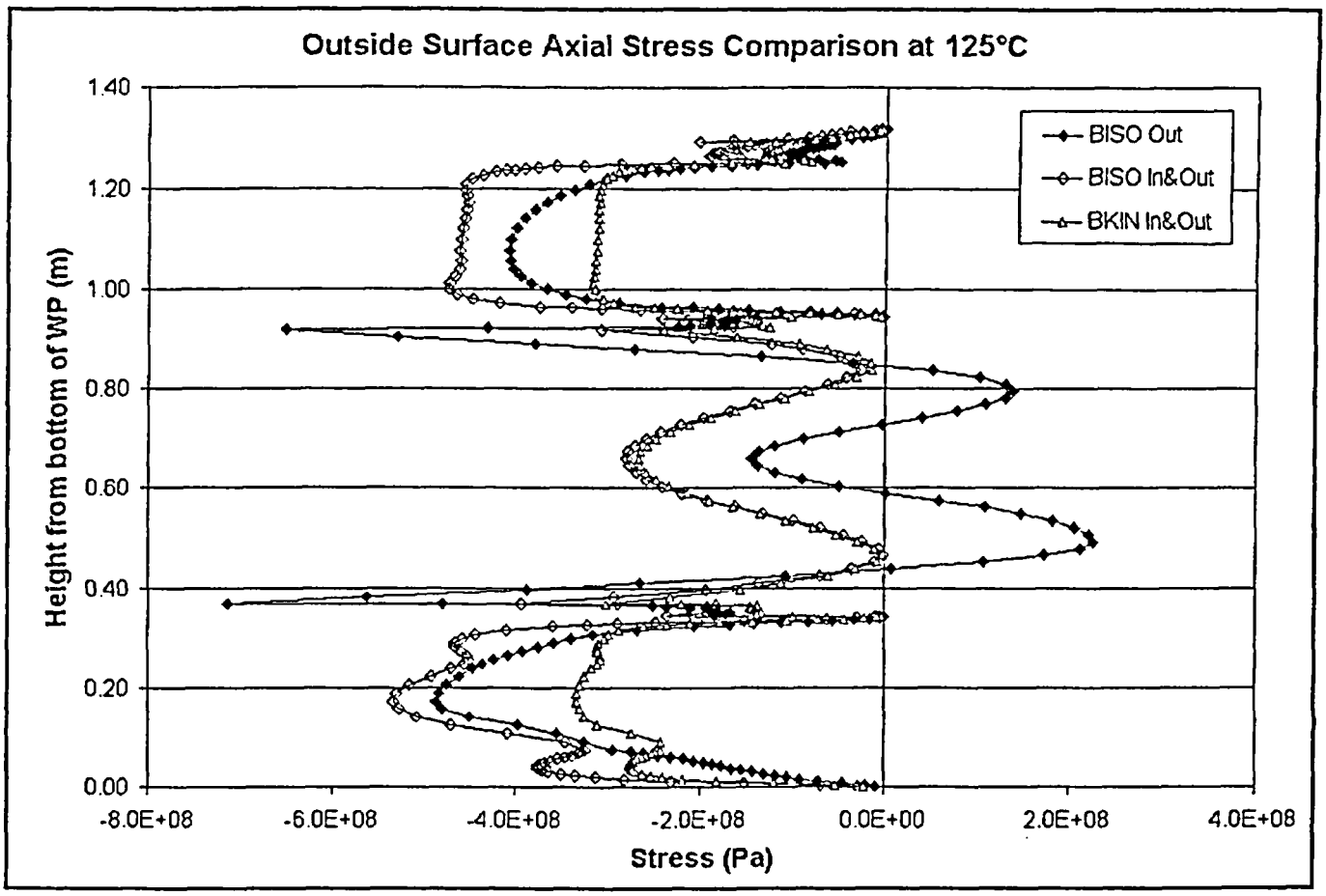

Figure 23: Outside Surface Axial Stress Comparison on the Side Wall of the WP at Operating Temperature of 125°C (Time = 1803 sec.)

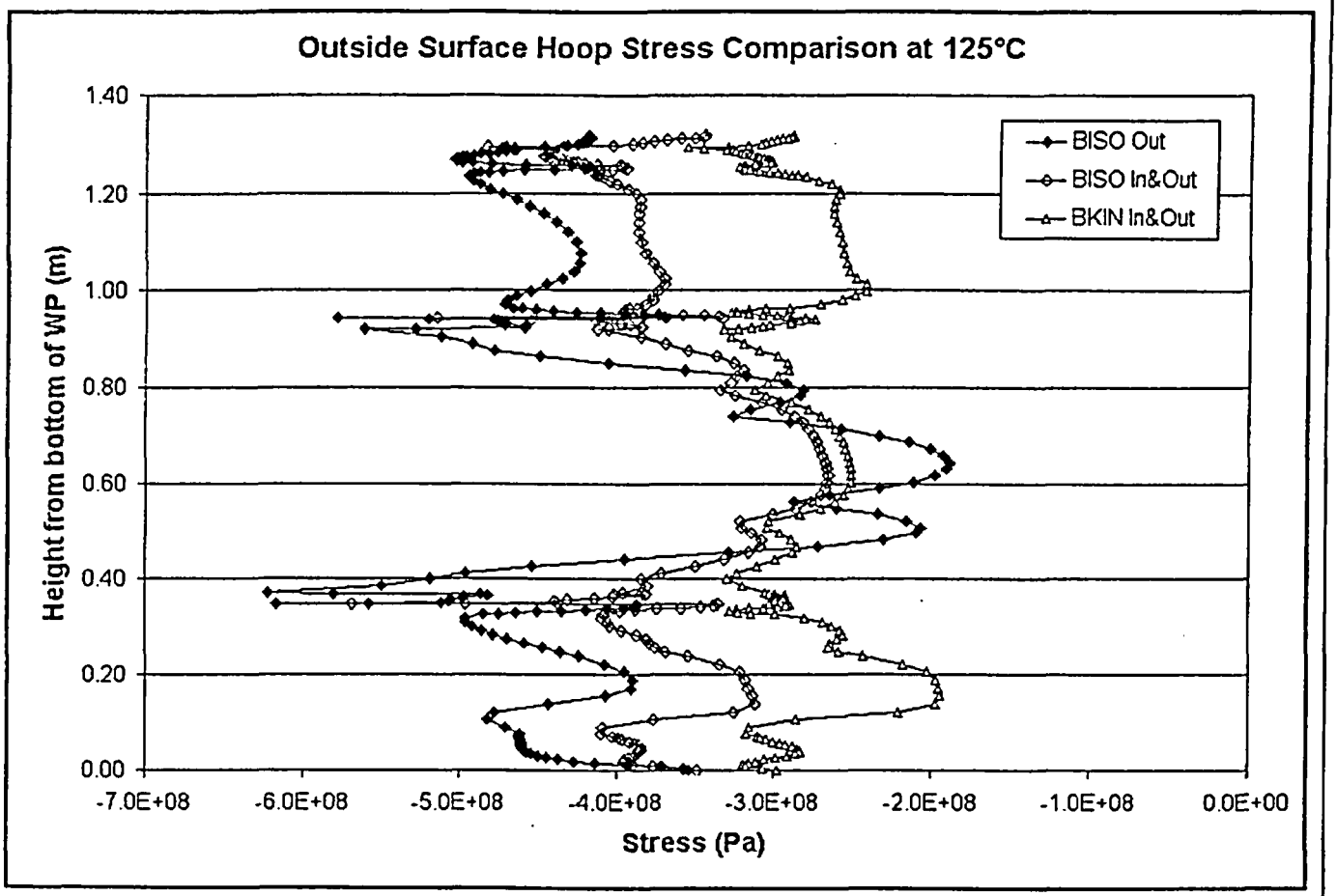

Figure 24: Outside Surface Hoop Stress Comparison on the Side Wall of the WP at Operating Temperature of 125°C (Time = 1803 sec.)

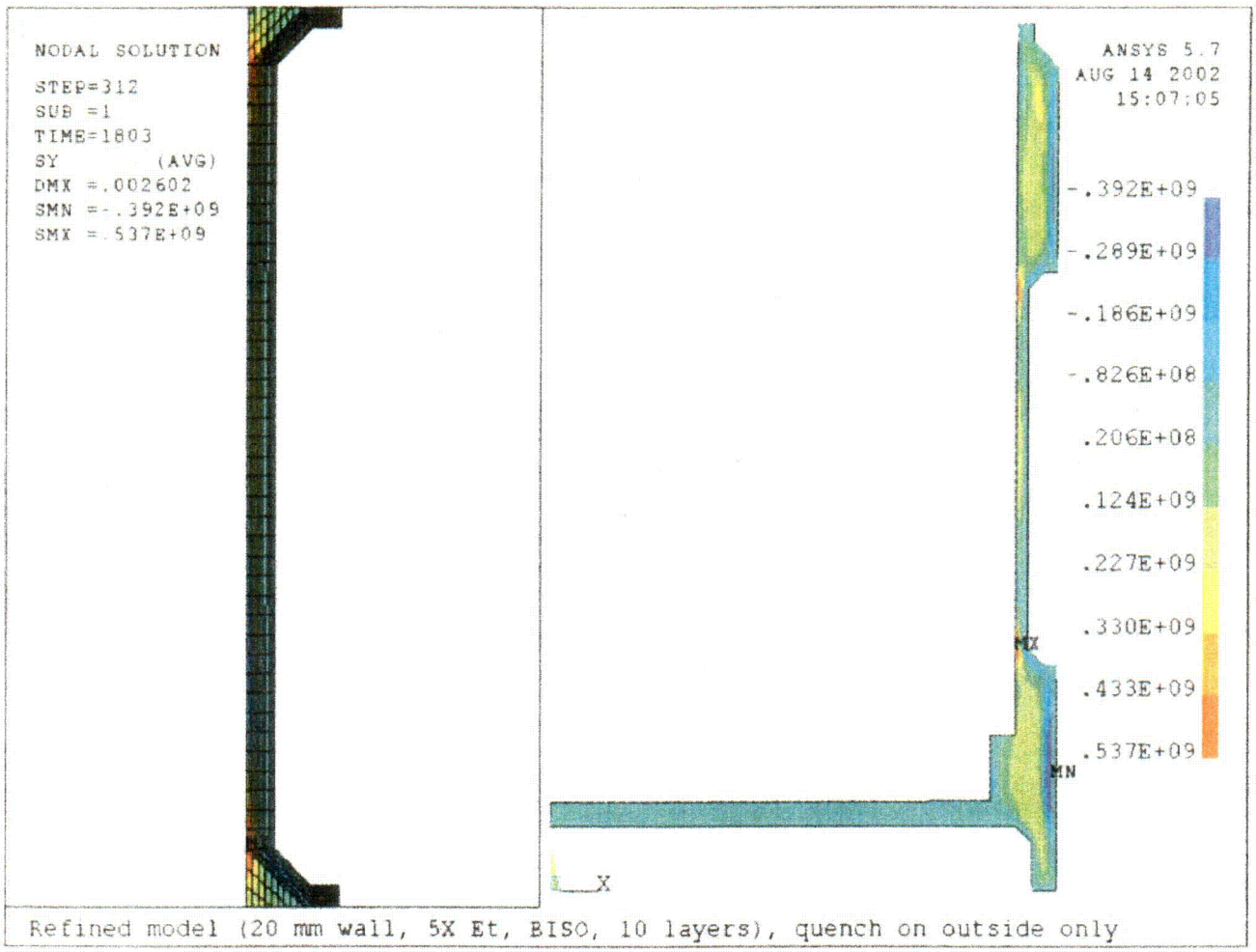

Figure 25: Axial Stress Plot for the Outside Quench Analysis Using BISO Curves at 125°C

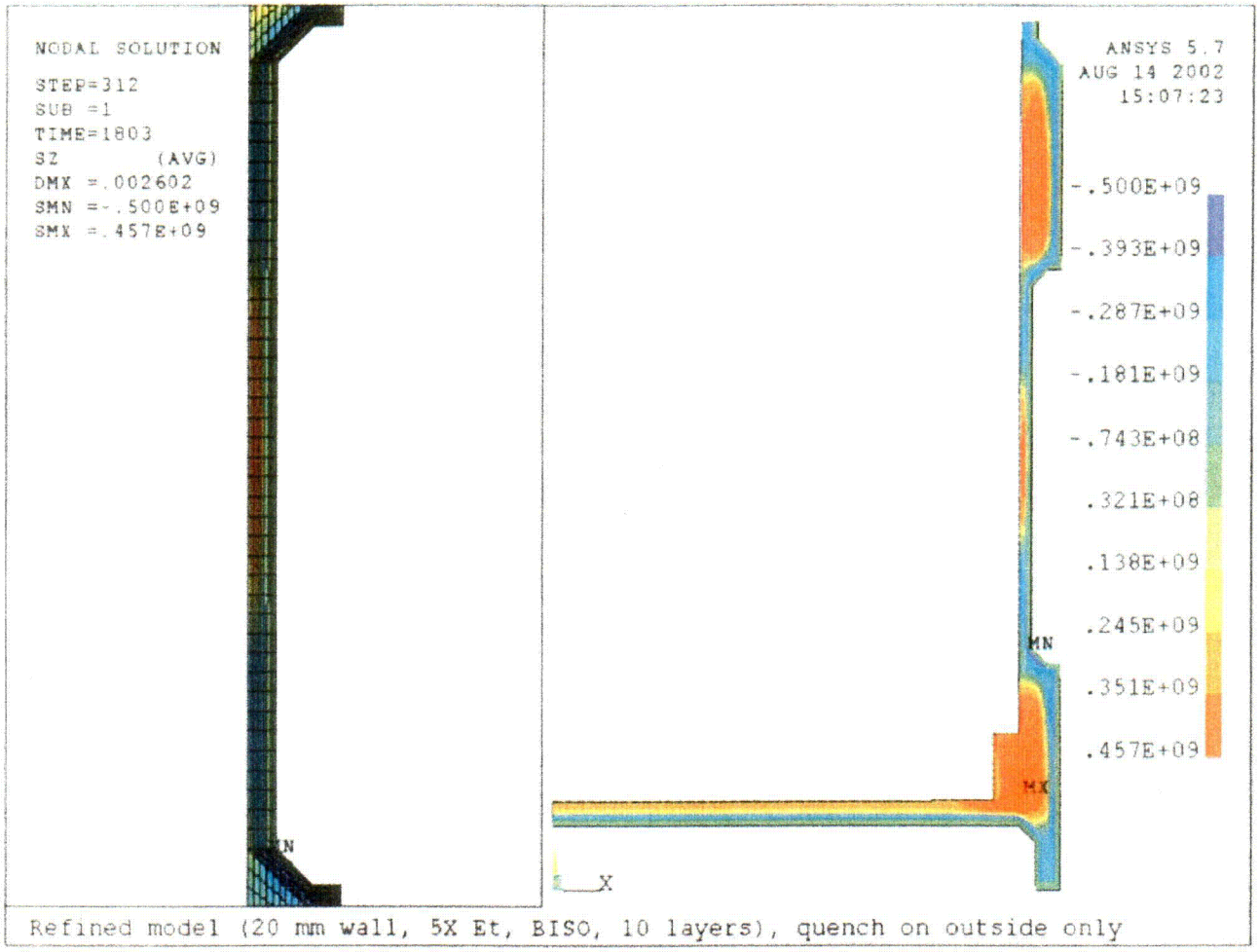

Figure 26: Hoop Stress Plot for the Outside Quench Analysis Using BISO Curves at 125°C

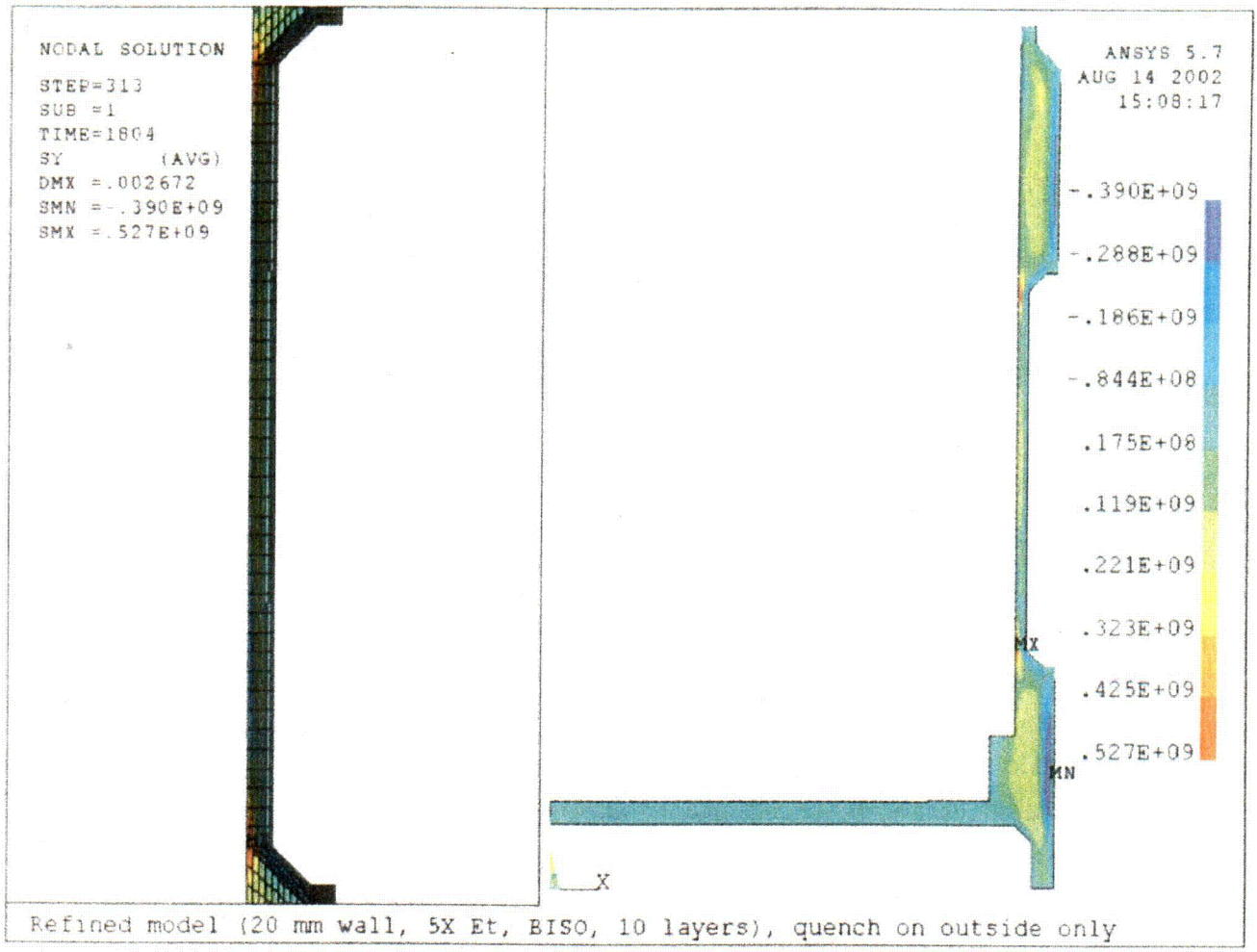

Figure 27: Axial Stress Plot After the First Layer is Removed, Outside Quench Using BISO Curves

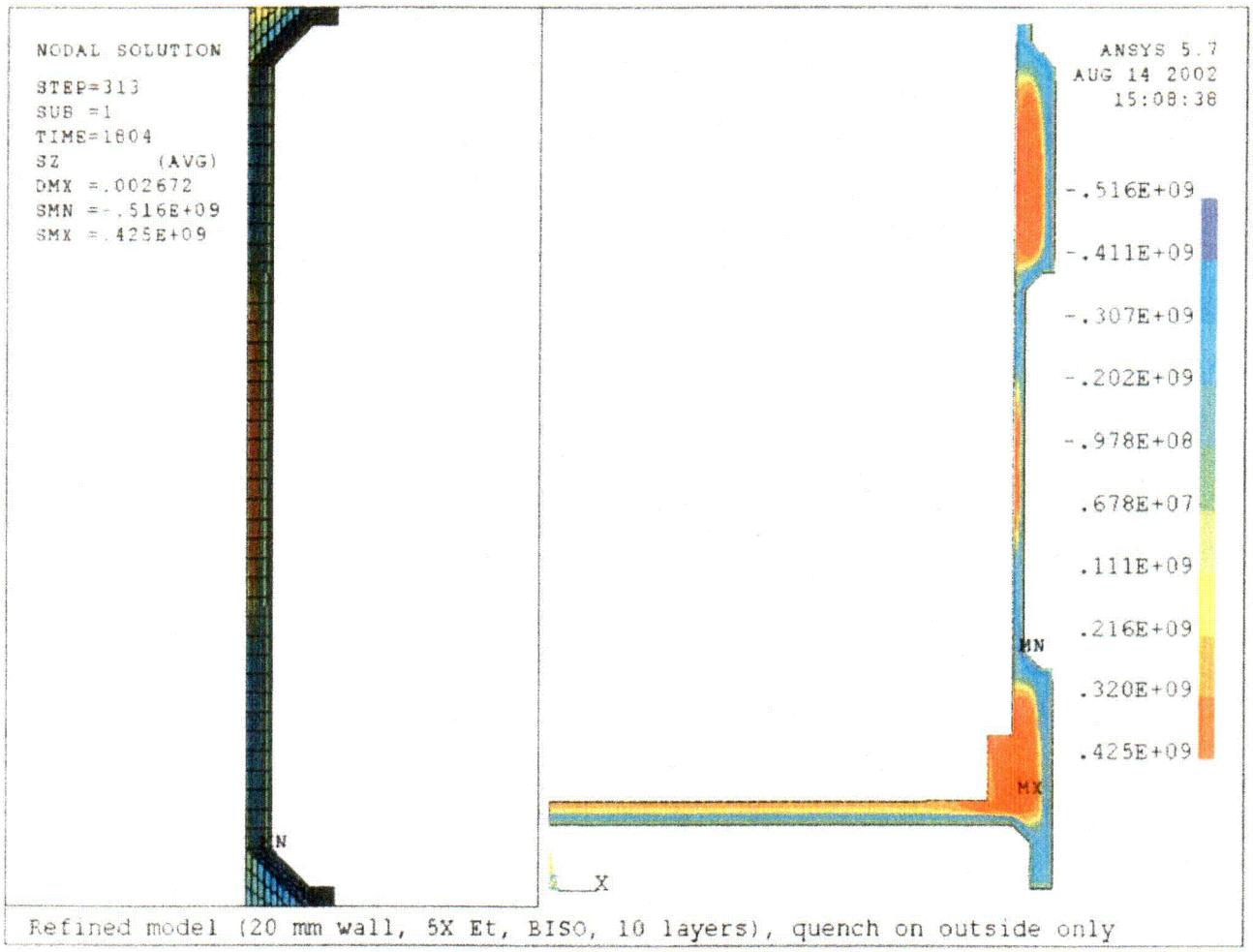

Figure 28: Hoop Stress Plot After the First Layer is Removed, Outside Quench Using BISO Curves

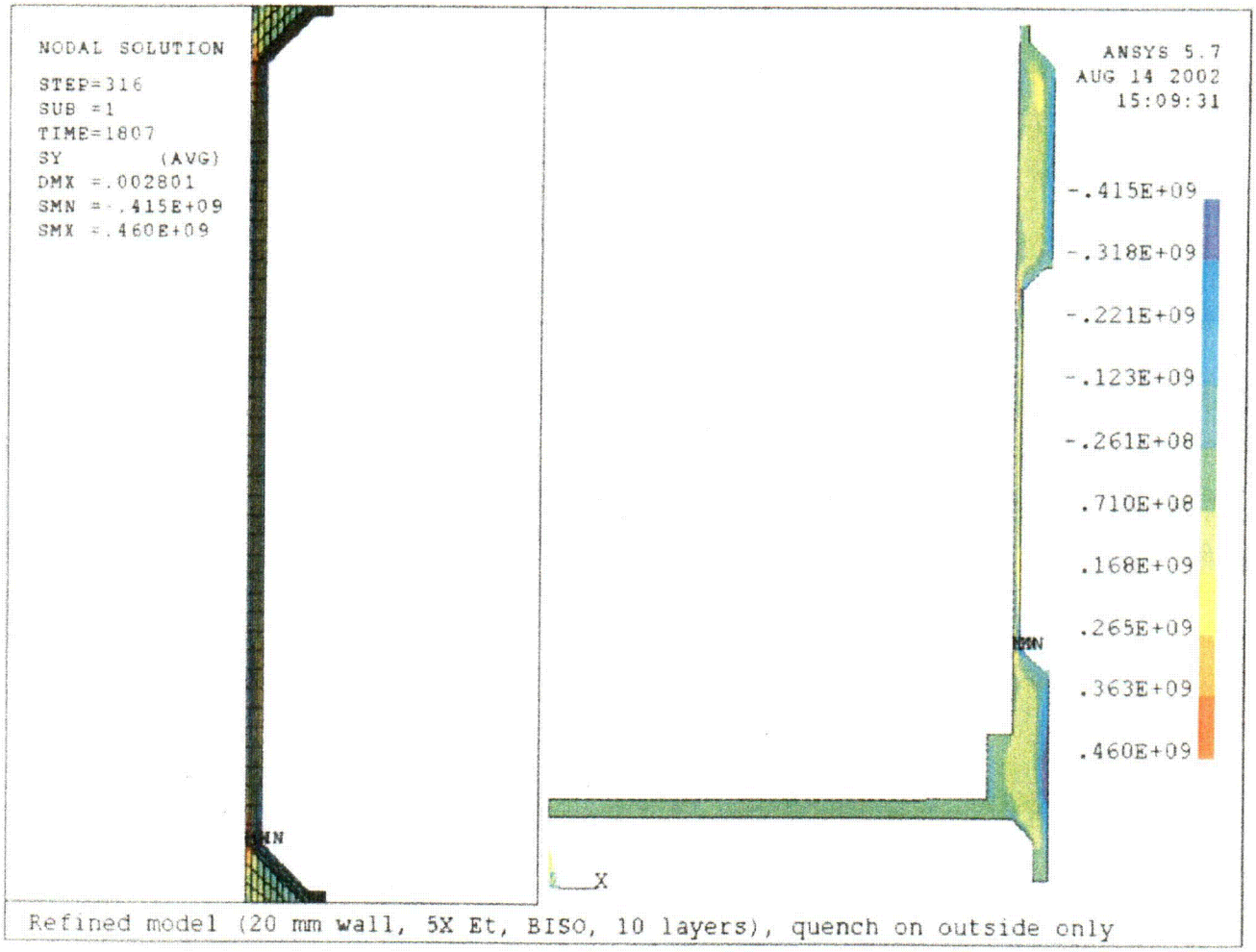

Figure 29: Axial Stress Plot After the Last Layer is Removed, Outside Quench Using BISO Curves

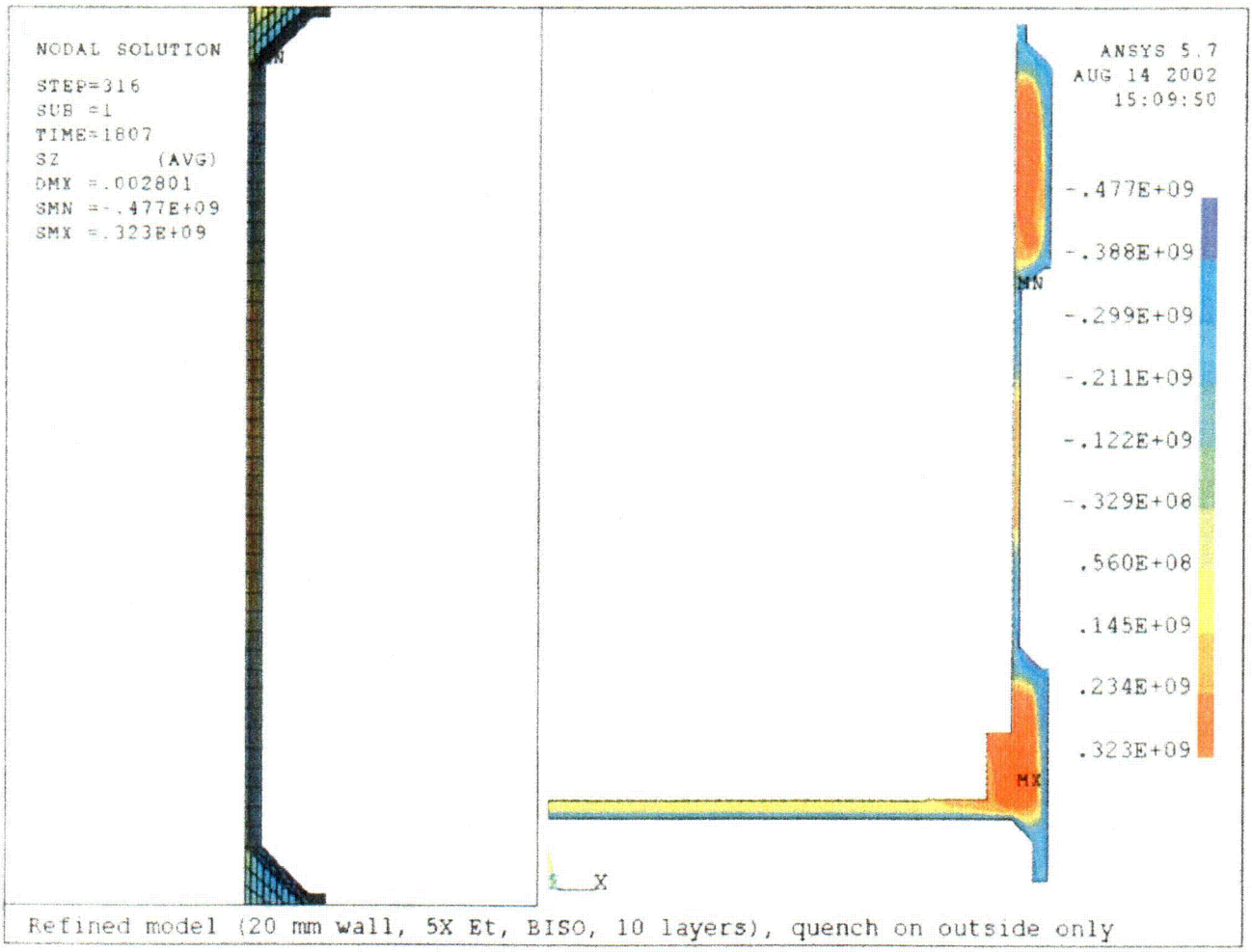

Figure 30: Hoop Stress Distribution After the Last Layer is Removed, Outside Quench Using BISO Curves

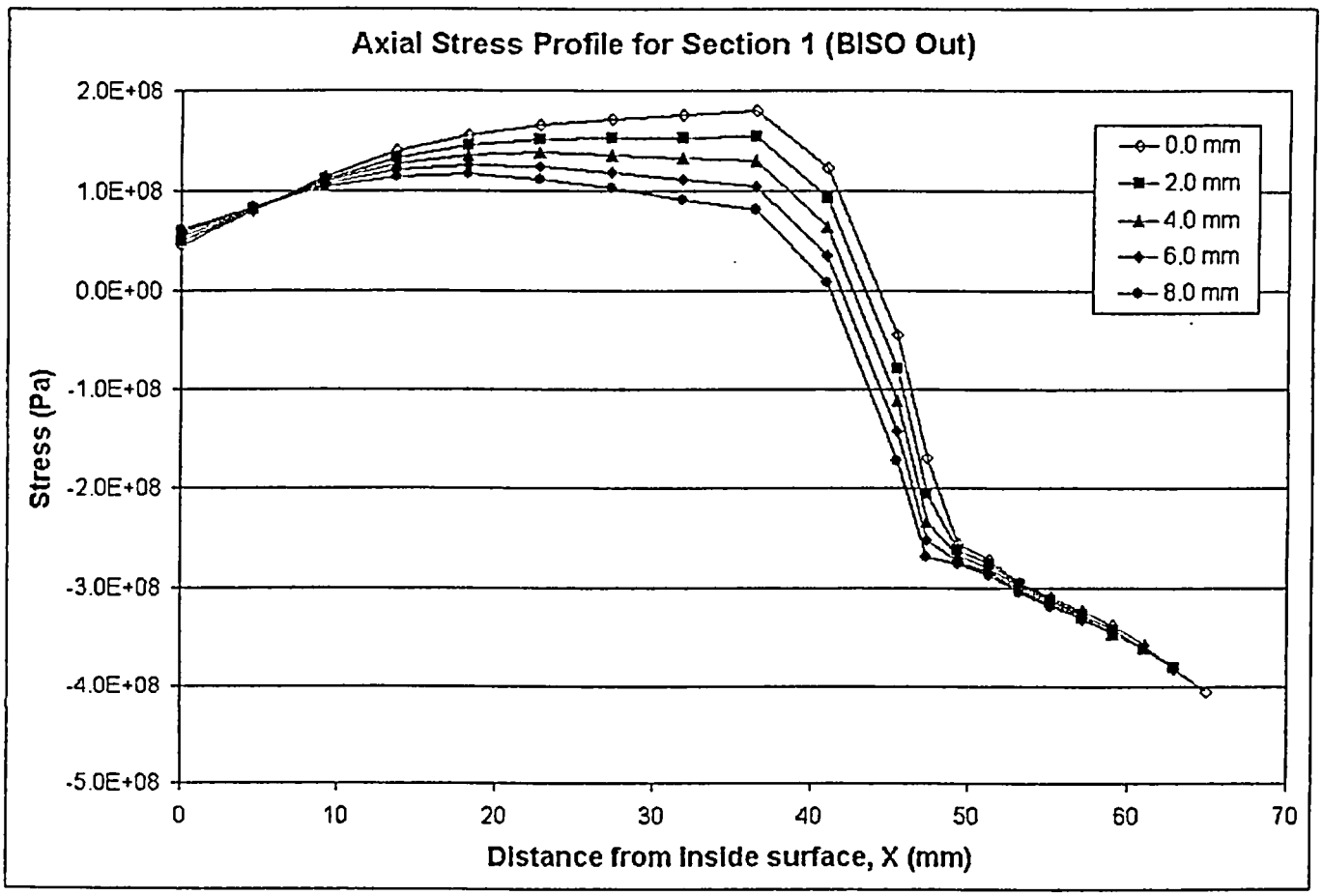

Figure 31: Through-Wall Axial Stresses for Section 1 for the Outside Quench Analysis Using BISO Curves

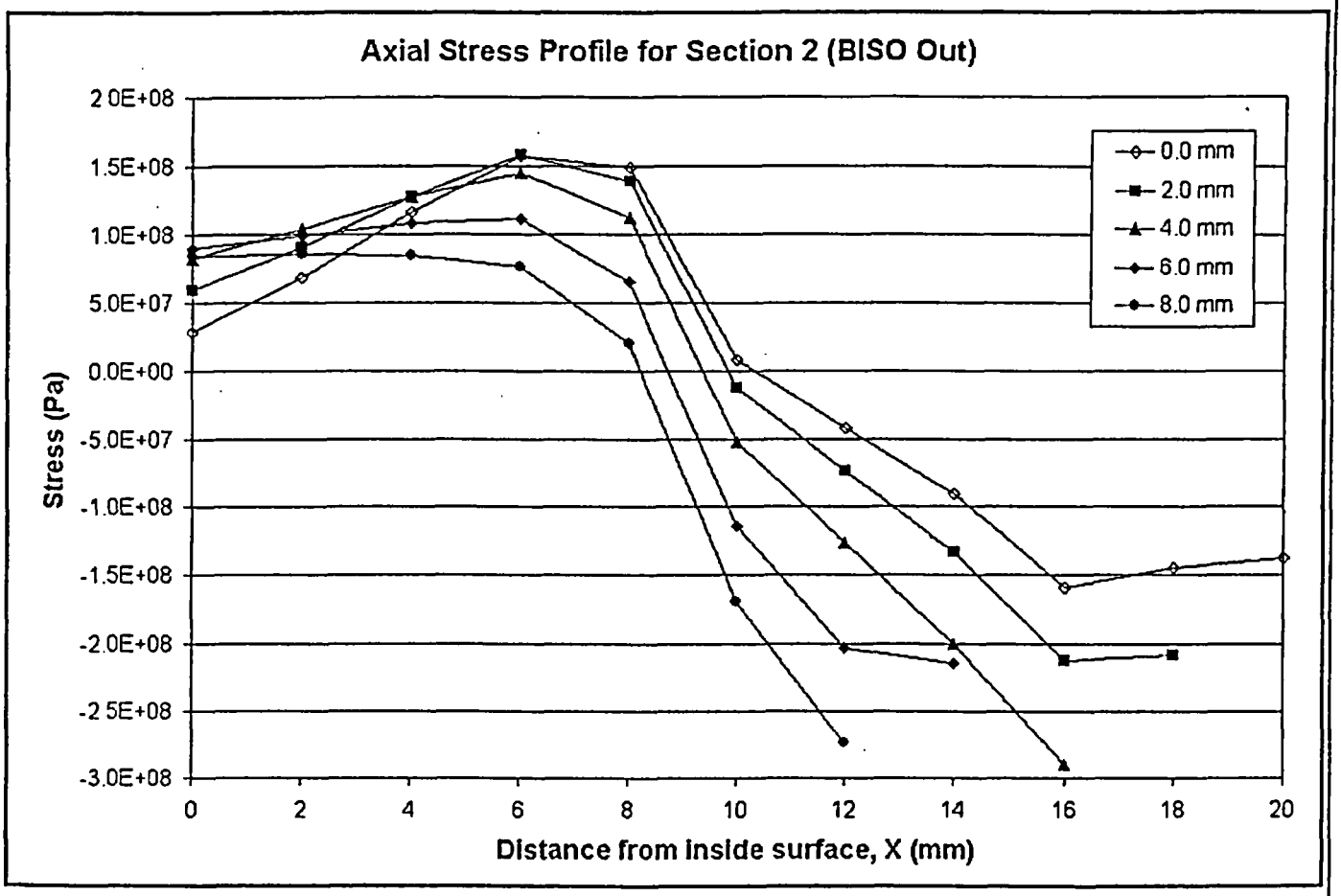

Figure 32: Through-Wall Axial Stresses for Section 2 for the Outside Quench Analysis Using BISO Curves

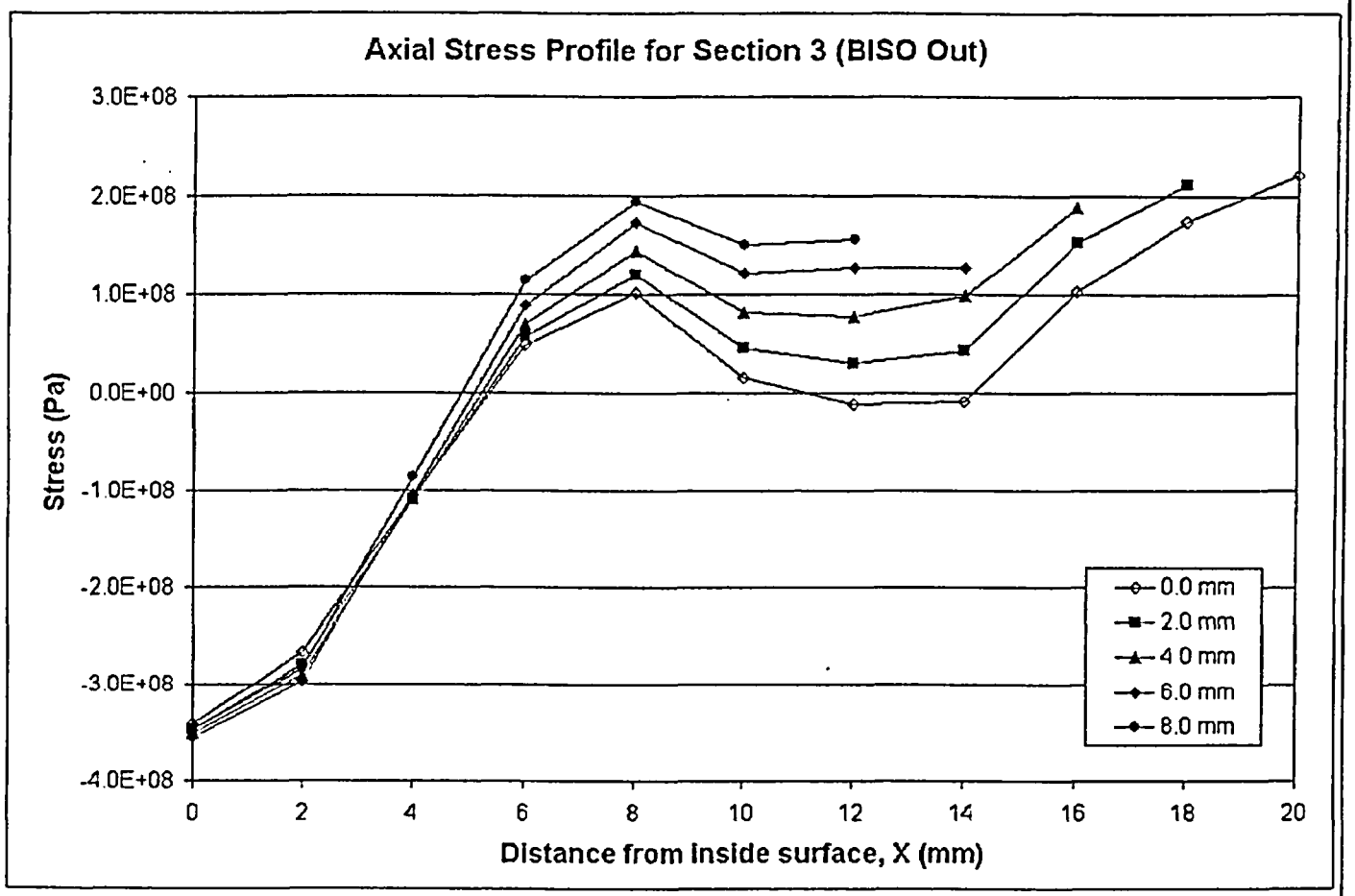

Figure 33: Through-Wall Axial Stresses for Section 3 for the Outside Quench Analysis Using BISO Curves

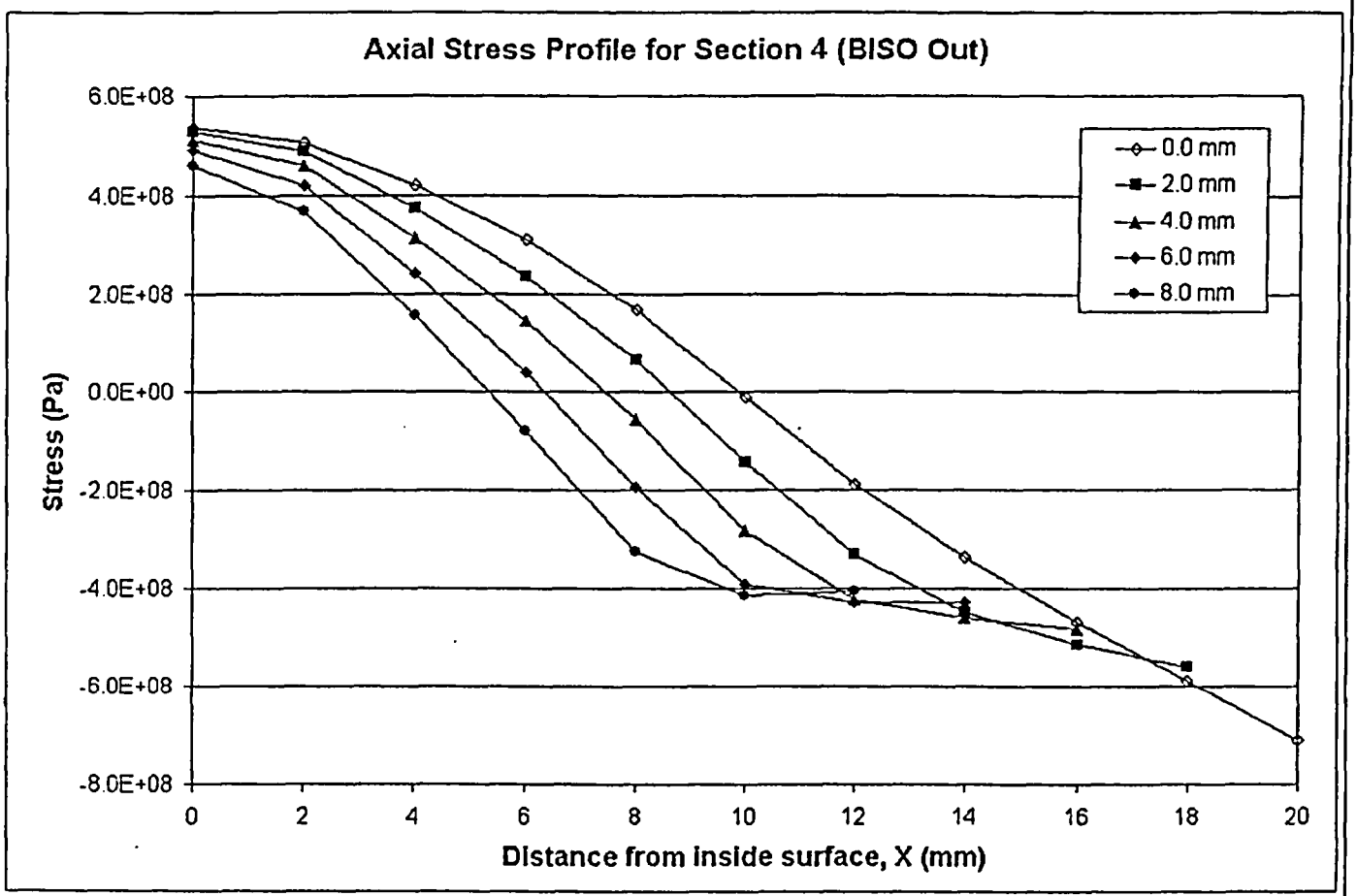

Figure 34: Through-Wall Axial Stresses for Section 4 for the Outside Quench Analysis Using BISO Curves

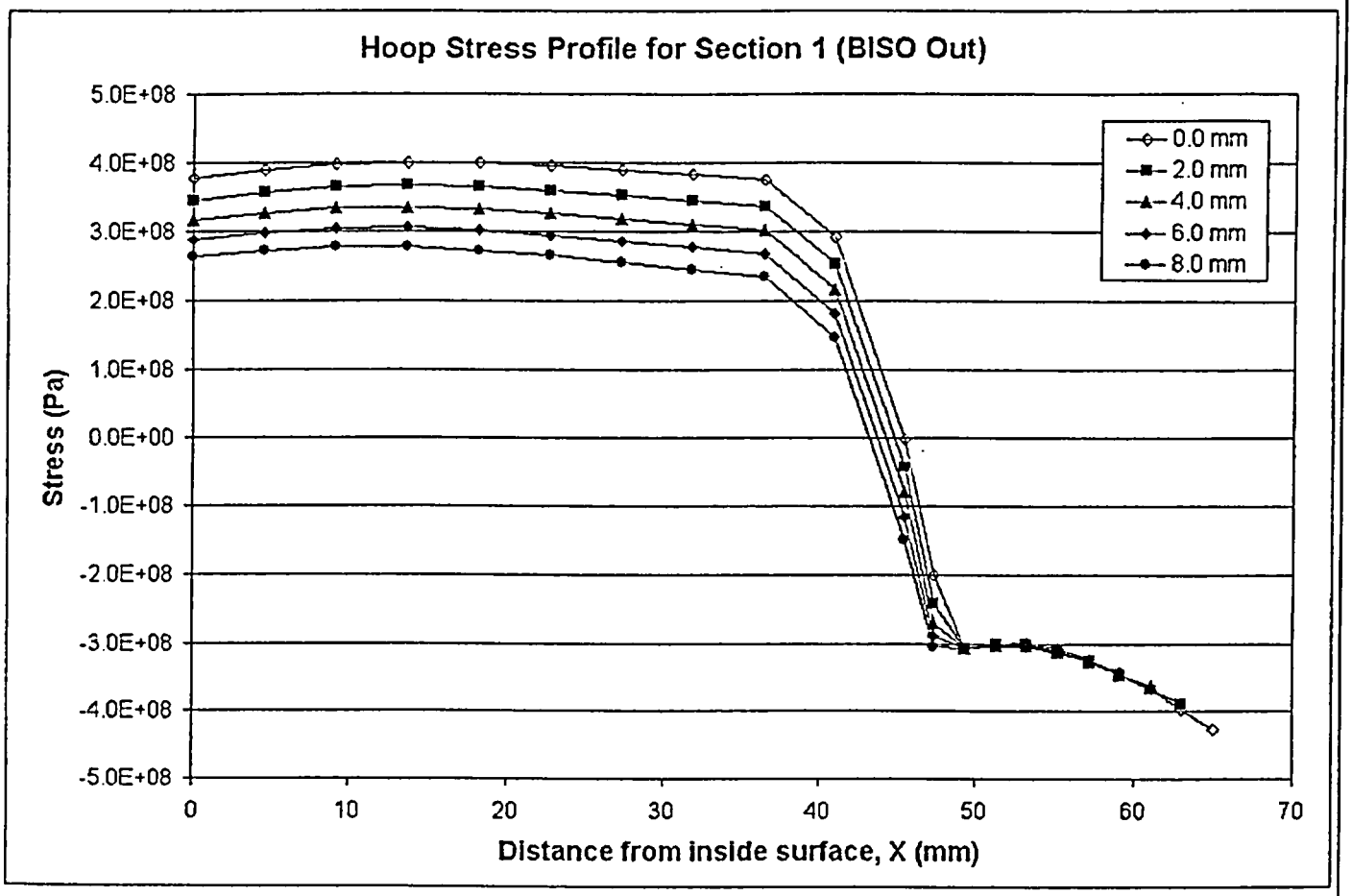

Figure 35: Through-Wall Hoop Stresses for Section 1 for the Outside Quench Analysis Using BISO Curves

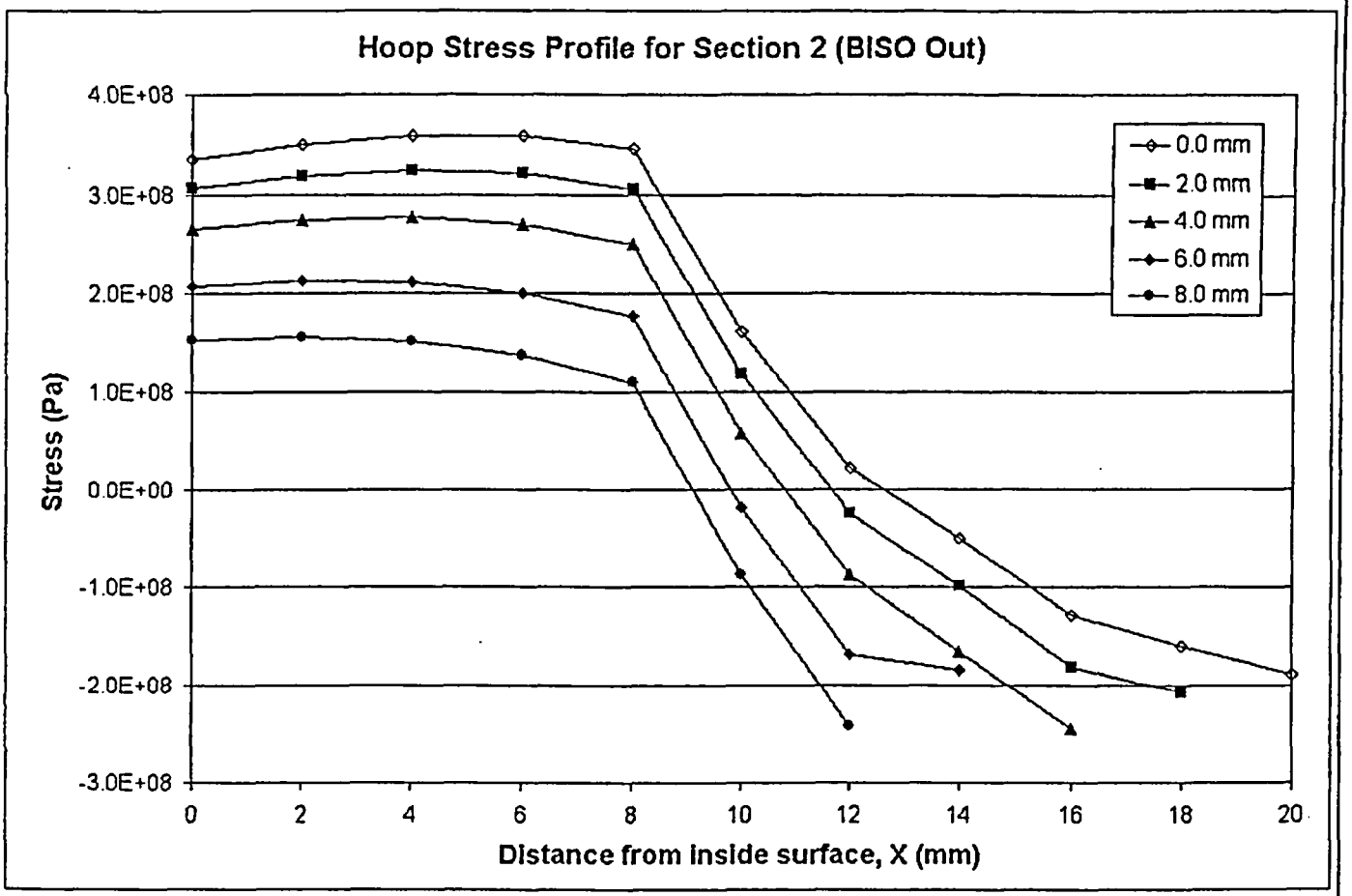

Figure 36: Through-Wall Hoop Stresses for Section 2 for the Outside Quench Analysis Using BISO Curves

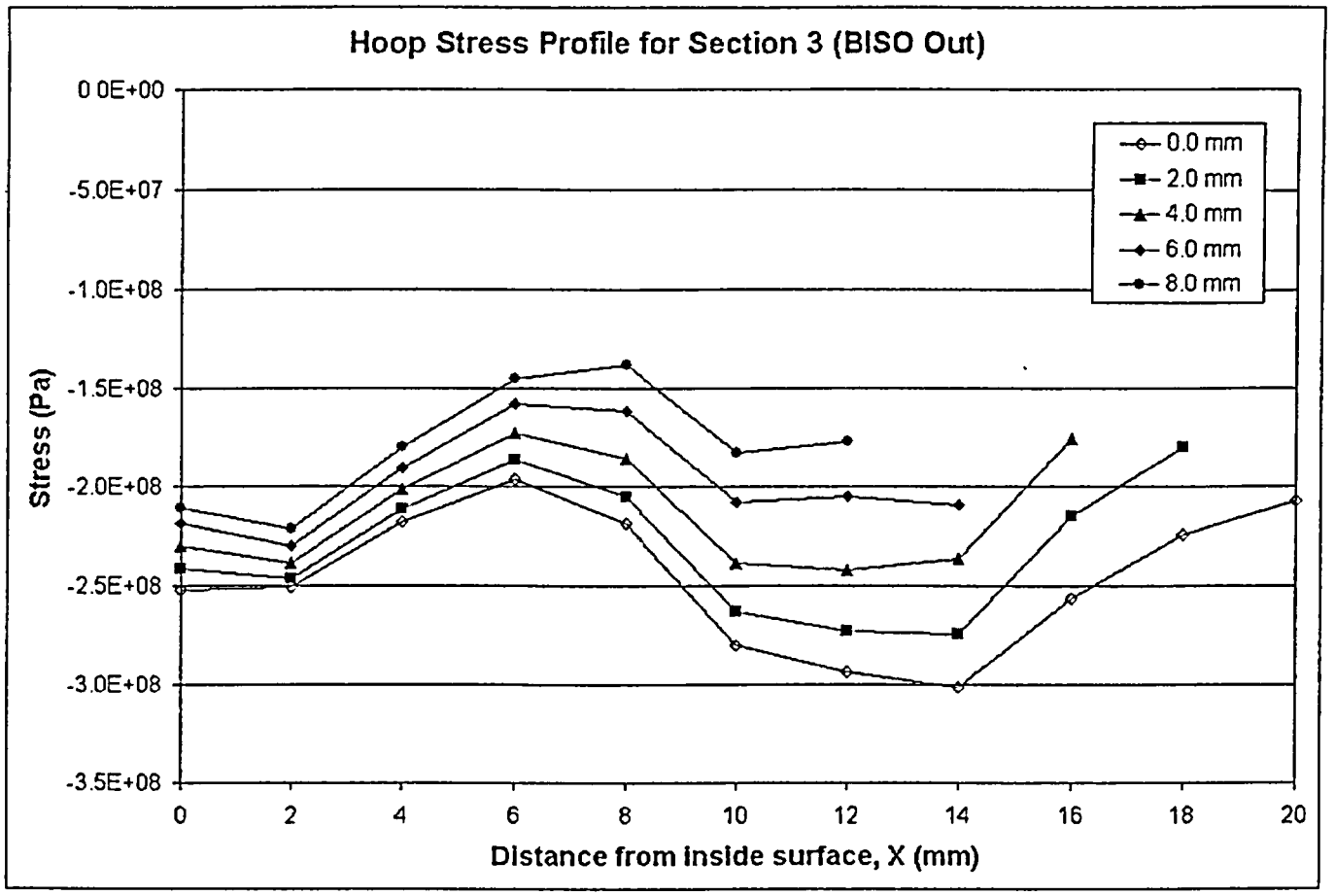

Figure 37: Through-Wall Hoop Stresses for Section 3 for the Outside Quench Analysis Using BISO Curves

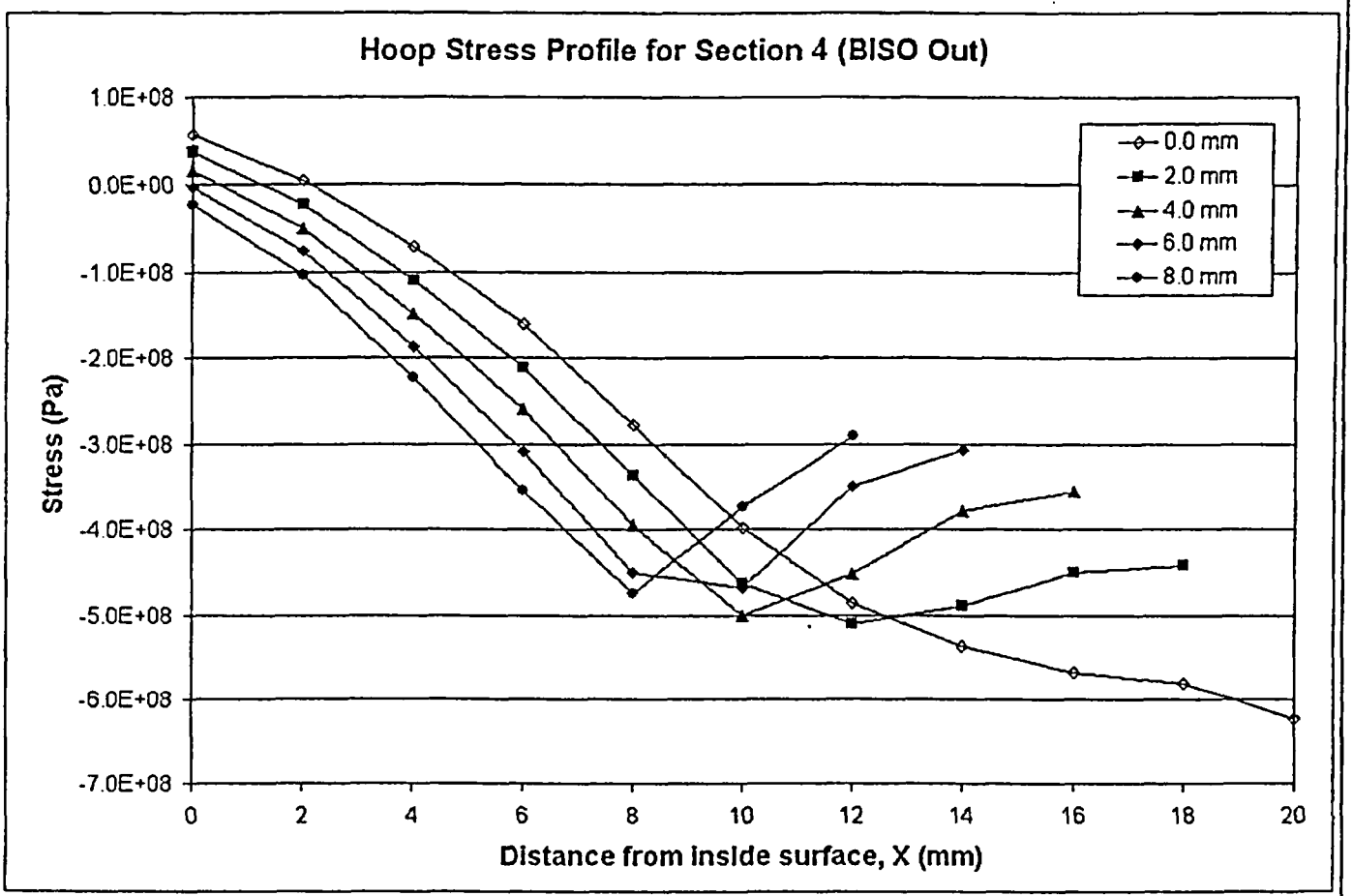

Figure 38: Through-Wall Hoop Stresses for Section 4 for the Outside Quench Analysis Using BISO Curves

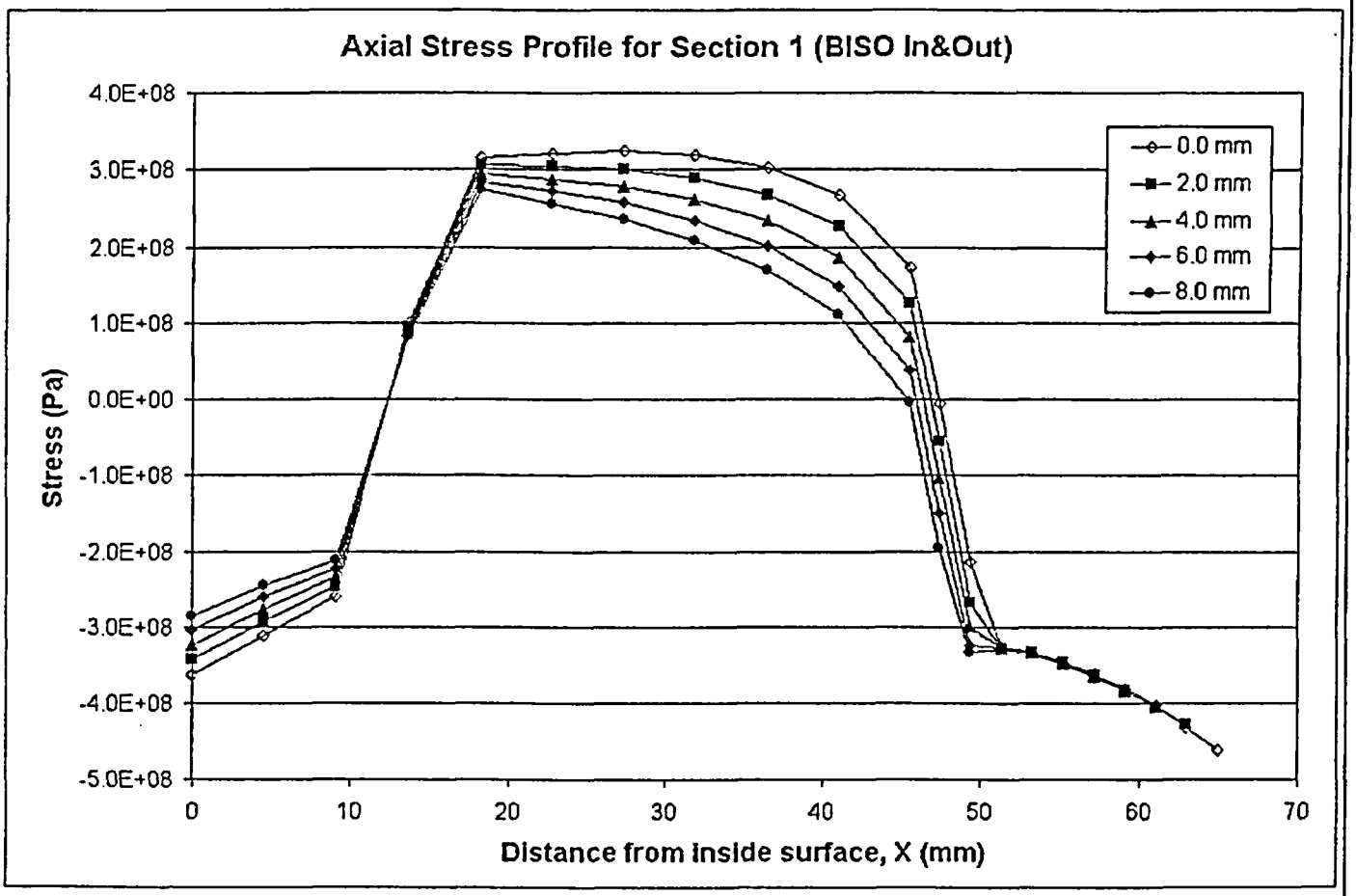

Figure 39: Through-Wall Axial Stresses for Section 1 for the Double-Sided Quench Analysis Using BISO Curves

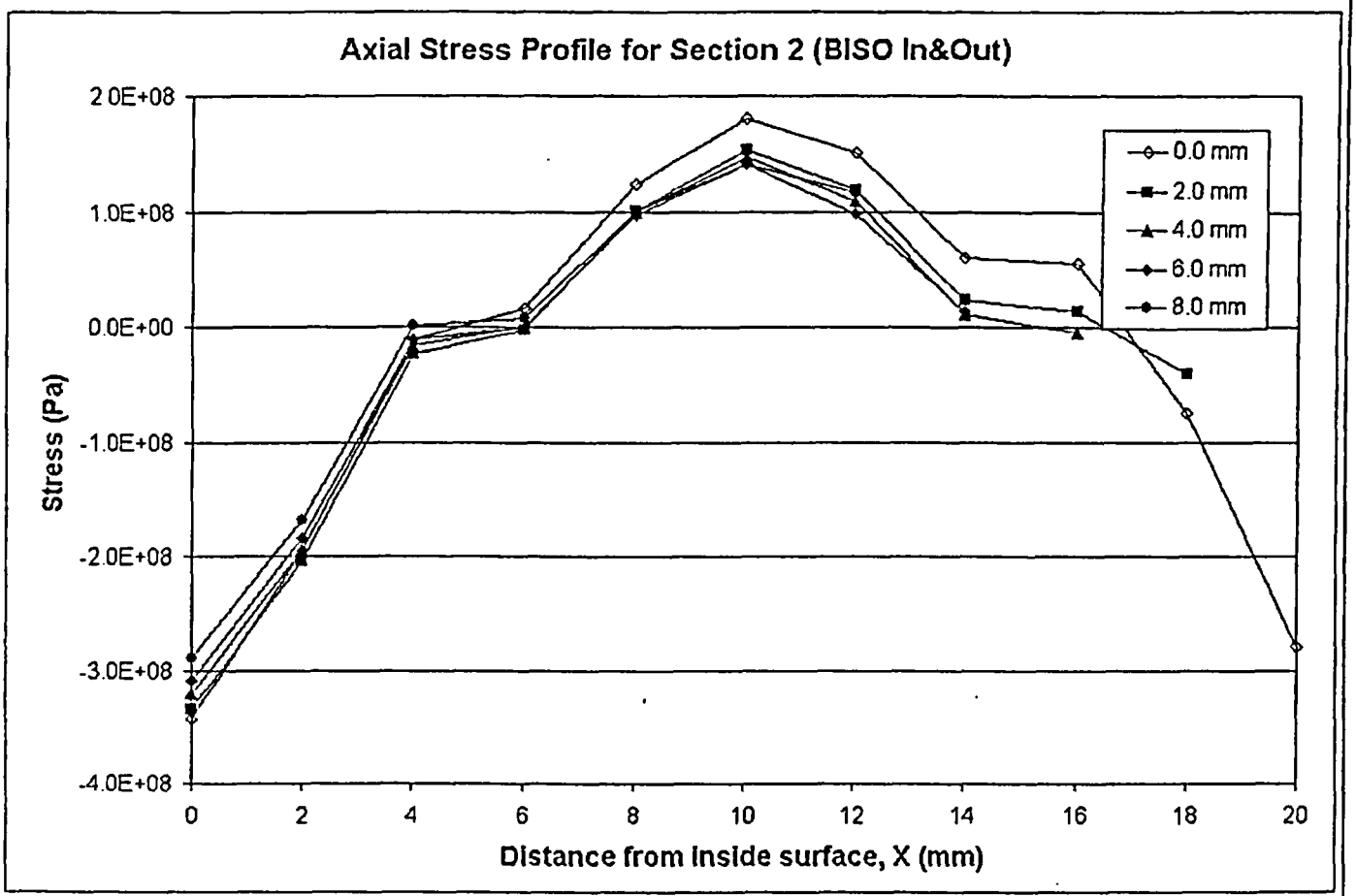

Figure 40: Through-Wall Axial Stresses for Section 2 for the Double-Sided Quench Analysis Using BISO Curves

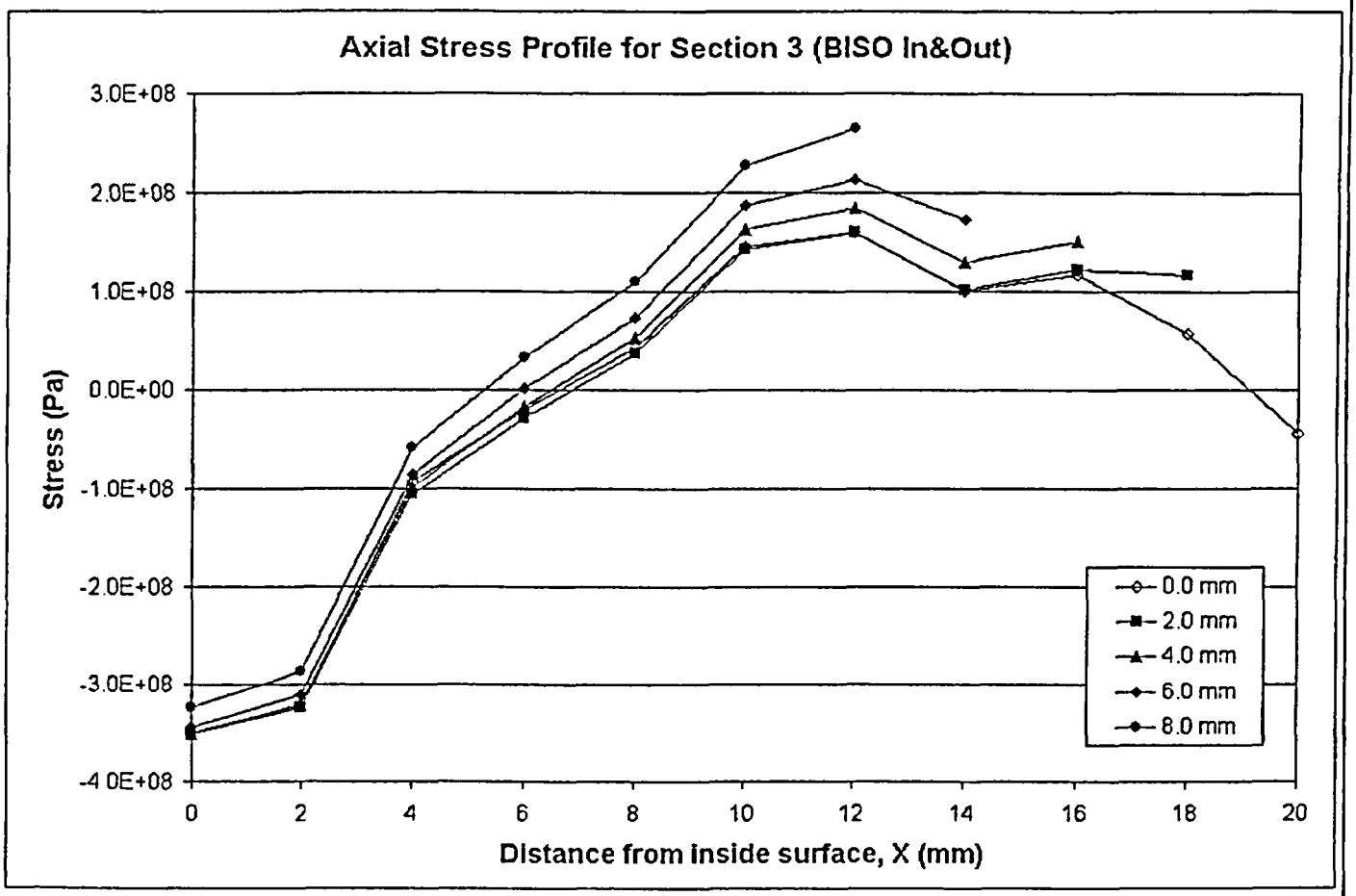

Figure 41: Through-Wall Axial Stresses for Section 3 for the Double-Sided Quench Analysis Using BISO Curves

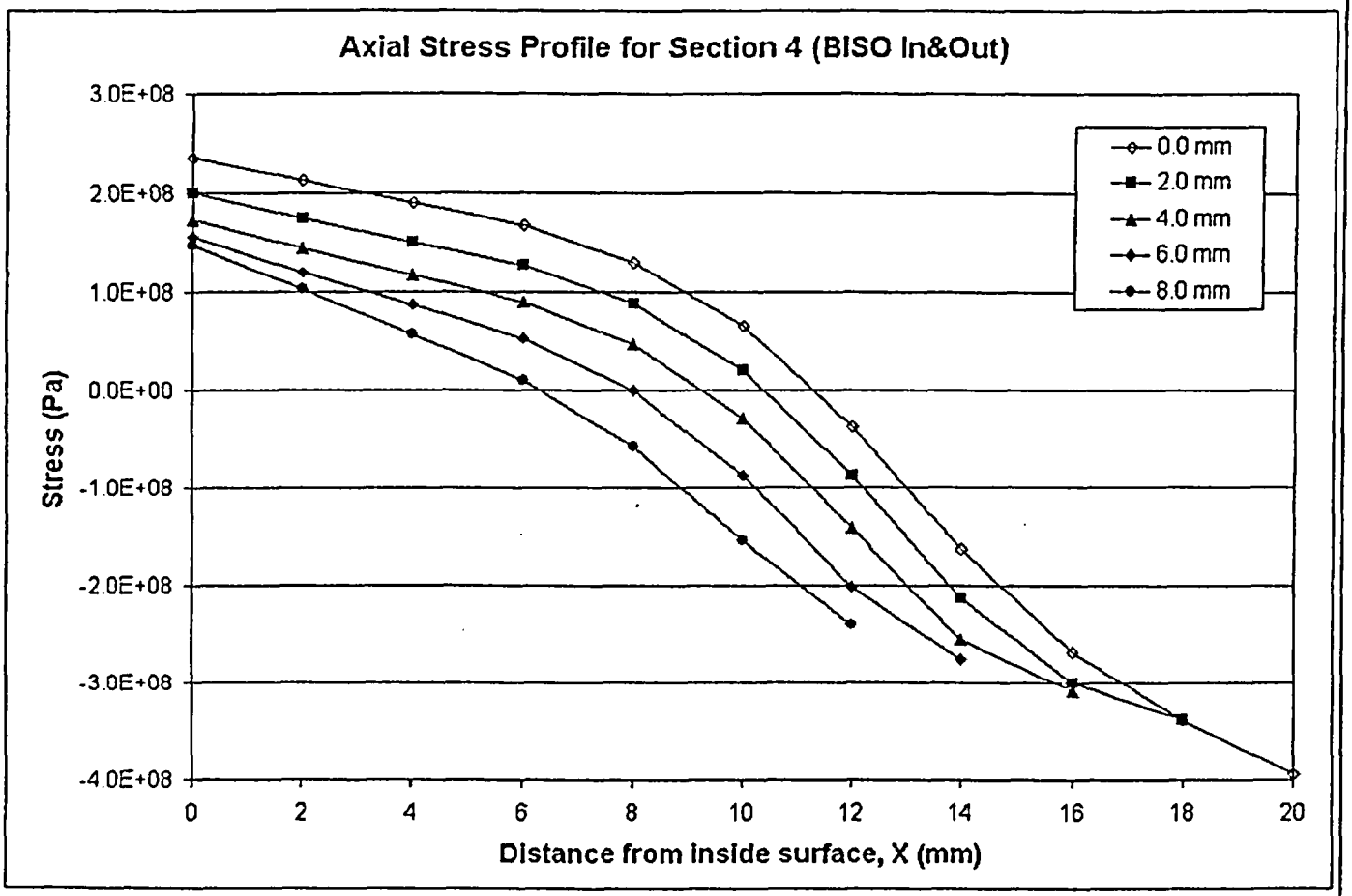

Figure 42: Through-Wall Axial Stresses for Section 4 for the Double-Sided Quench Analysis Using BISO Curves

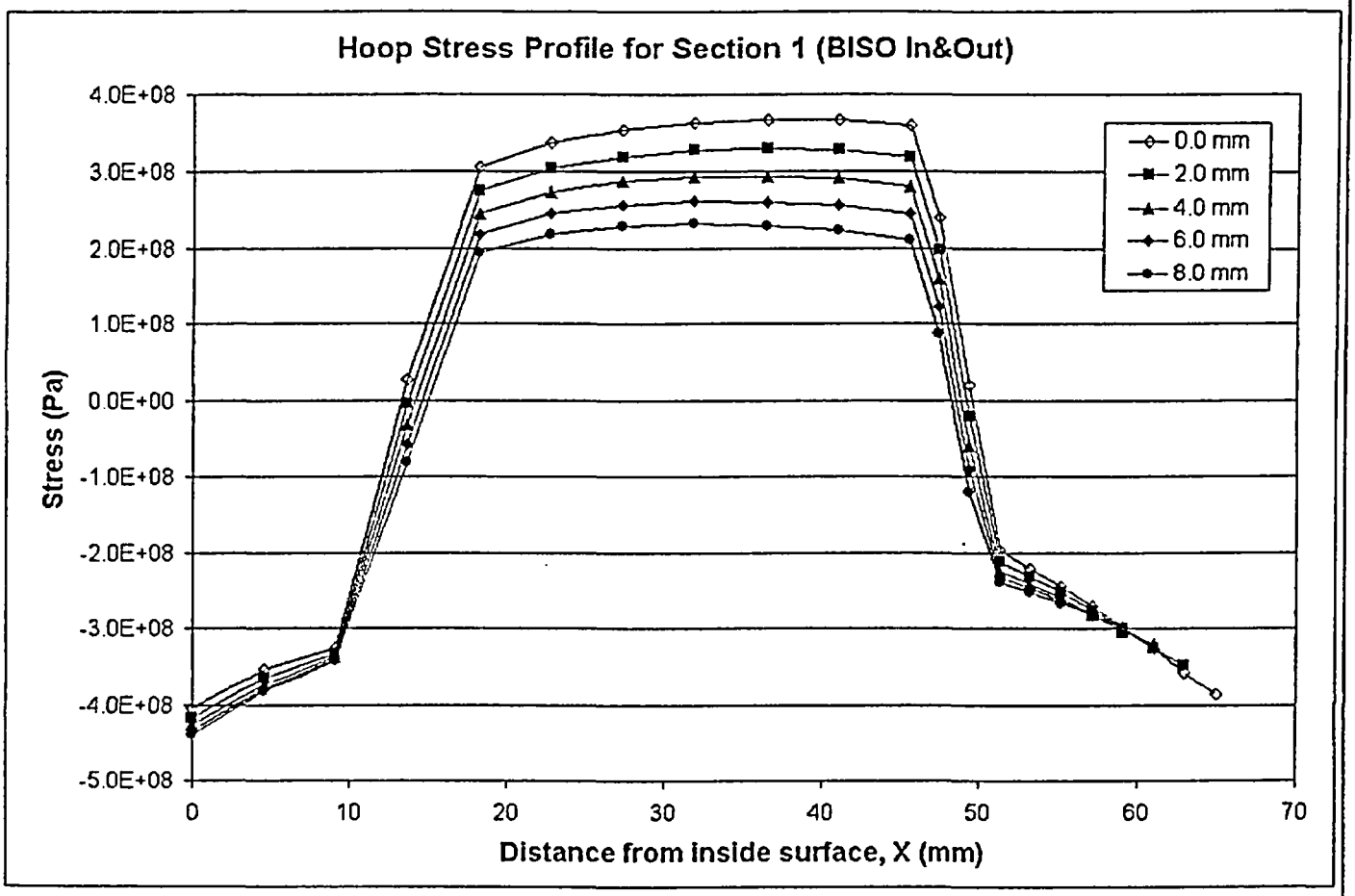

Figure 43: Through-Wall Hoop Stresses for Section 1 for the Double-Sided Quench Analysis Using BISO Curves

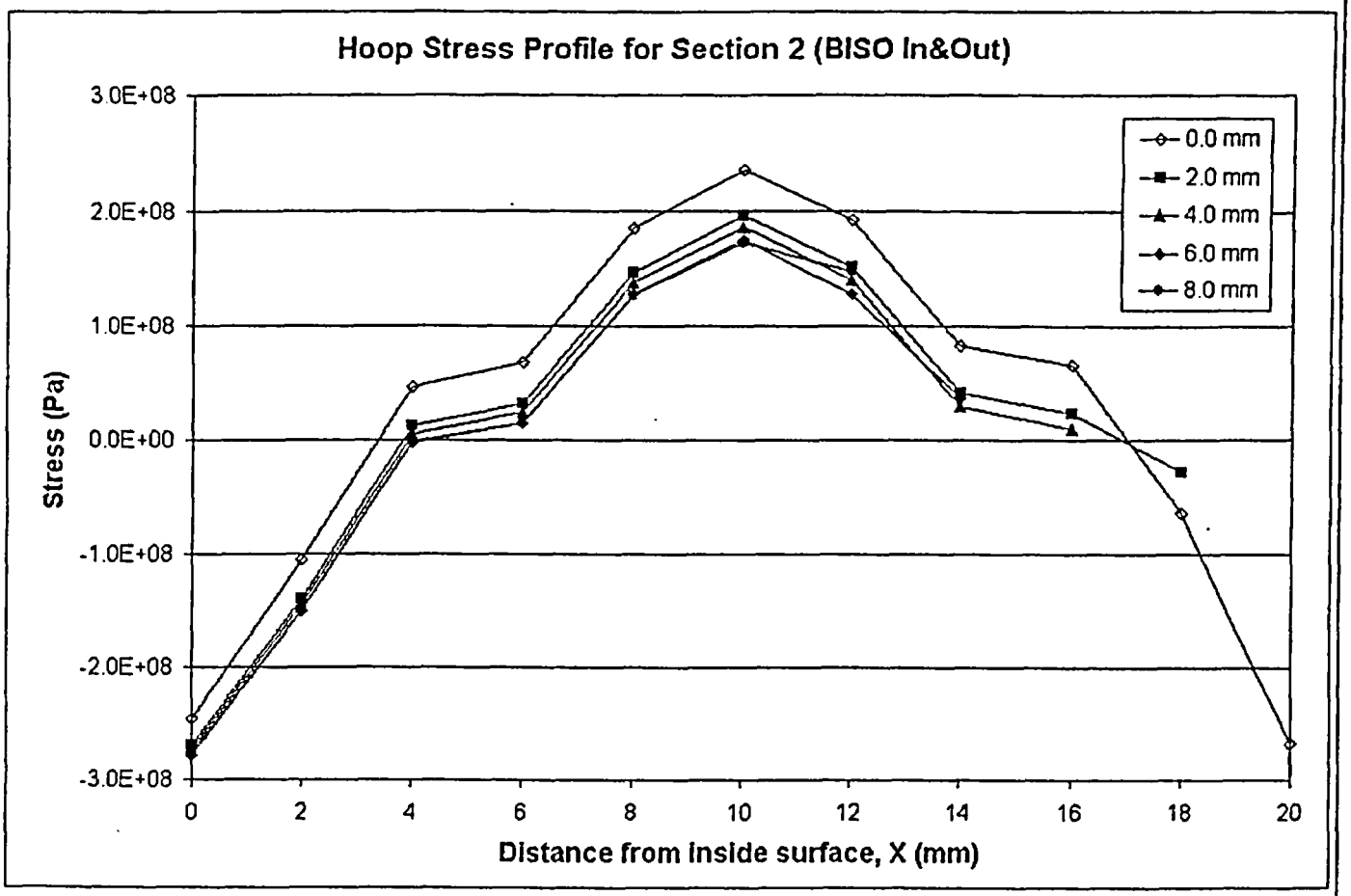

Figure 44: Through-Wall Hoop Stresses for Section 2 for the Double-Sided Quench Analysis Using BISO Curves